BOUNTY GOLD MINE : DEFORMATION HISTORY AND THE DEVELOPMENT OF ORE FLUID PATHWAYS WITHIN AN IRON FORMATION HOST, WESTERN AUSTRALIA

Alexander

by Robert A. Rutherford

1993

This thesis is submitted as partial fulfillment of the
Degree of Master in Economic Geology, University of Tasmania

ABSTRACT

The Bounty orebody has a steep plunge and is bound within strata parallel shear zones which are developed in an iron formation horizon. A footwall ultramafic volcanic sequence and a hanging wall gabbro bound the mineralized iron formation which dips steeply west. Shearing occurred during deformation event Dn and a peak contact metamorphic grade of lower amphibolite facies.

Deformation in pre–Dn times was dominated by strong east–west directed compression which resulted in complex, upright folding and thrusting of the supracrustal sequence. With cessation or relaxation of the compression batholiths, plutons and porphyritic stocks, dykes and sills of granite to granodiorite composition intruded the folded greenstone sequence and broad contact metamorphic aureoles were formed. A period of vertically oriented, maximum compressive stress (Dn) succeeded the intrusive event. Resulting strain was focused along the footwall and hanging wall boundaries of the iron formation and shear zones with a normal movement sense developed. The hanging wall boundary of the iron formation, which was locally rotated west of north during intrusion of a pre–Dn pluton, underwent down dip or steep oblique shear movement with a normal sense. Sheared lithological boundaries striking about 4° to 8° west of north were dilated, developing ore fluid pathways with a steep plunge.

The ore fluid pathways are controlled by the rheological contrast and original shape of the iron formations hanging wall boundary during Dn. The original shape was influenced by intrusion of a pre–Dn pluton proximal to the deposit.

CONTENTS

CONTENTS
Page 2

LIST OF FIGURES

LIST OF FIGURES
Page 2

LIST OF FIGURES
Page 3

LIST OF FIGURES
Page 4

APPENDICES

INTRODUCTION

The Bounty deposit is an Archaean gold-lode hosted within an amphibolite facies greenstone sequence. The orebody is stratabound within a sheared iron formation, steep plunging and contains greater than 1 million ounces of gold. Since the discovery of mineralization in 1986, a proved and probable reserve of 5.3 million tonnes at 7.1g/t gold has been outlined to a depth of about 900 metres below surface. The deposit is open at depth.

The mine is located 360 kilometres east of Perth in the Forrestania Greenstone Belt (Chin et al., 1984), Yilgarn Block, Western Australia (Fig. 1 and Fig. 2). This belt forms the southern extension to the Southern Cross Greenstone Belt (Gee, 1979) which also contains Archaean gold-lodes hosted in amphibolite facies rocks (Fig. 2). These deposits in the Southern Cross Belt are described as high-temperature Archaean gold skarns formed during contact metamorphic conditions of amphibolite facies (Mueller, 1988; Mueller, 1991; Mueller et al., 1991; Mueller and Groves, 1991). Unlike the Southern Cross deposits, the Bounty deposit has no significant tectonic events overprinting mineralization which has enabled it to be confidently constrained within the regional tectonic framework.

This study follows Caswell's (1989) initial petrographic documentation and geochemical study of mineralization at the Bounty Gold Mine, and aims to define structural elements controlling gold mineralization within the deposit. To this end, the study documents the geological setting, igneous history, metamorphic history, vein history and gold mineralization with reference to deformation history on both regional and mine scales.

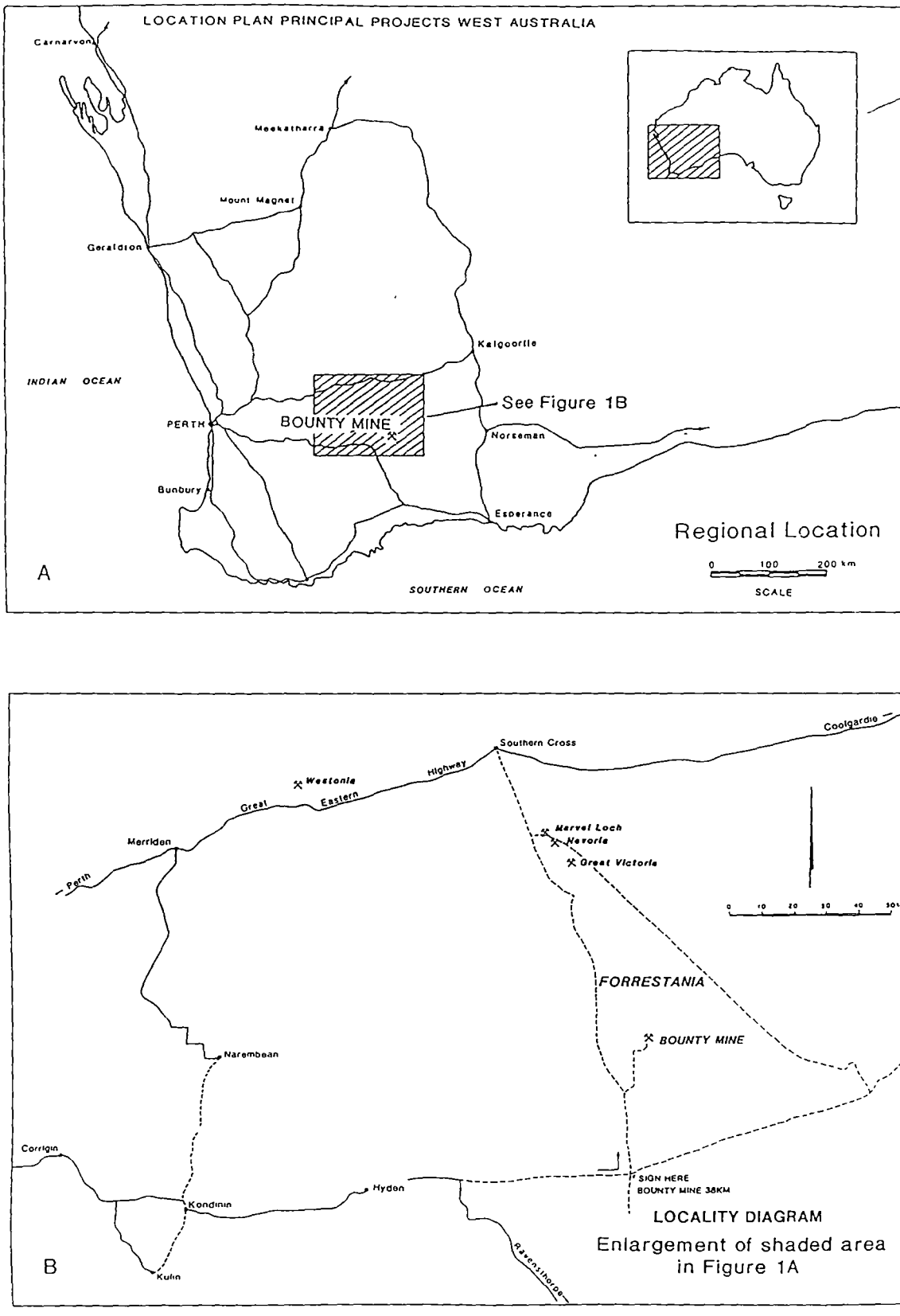

Figure 1: Location of the Bounty Gold Mine. Adapted from Aztec Mining Company Limited unpublished reports.

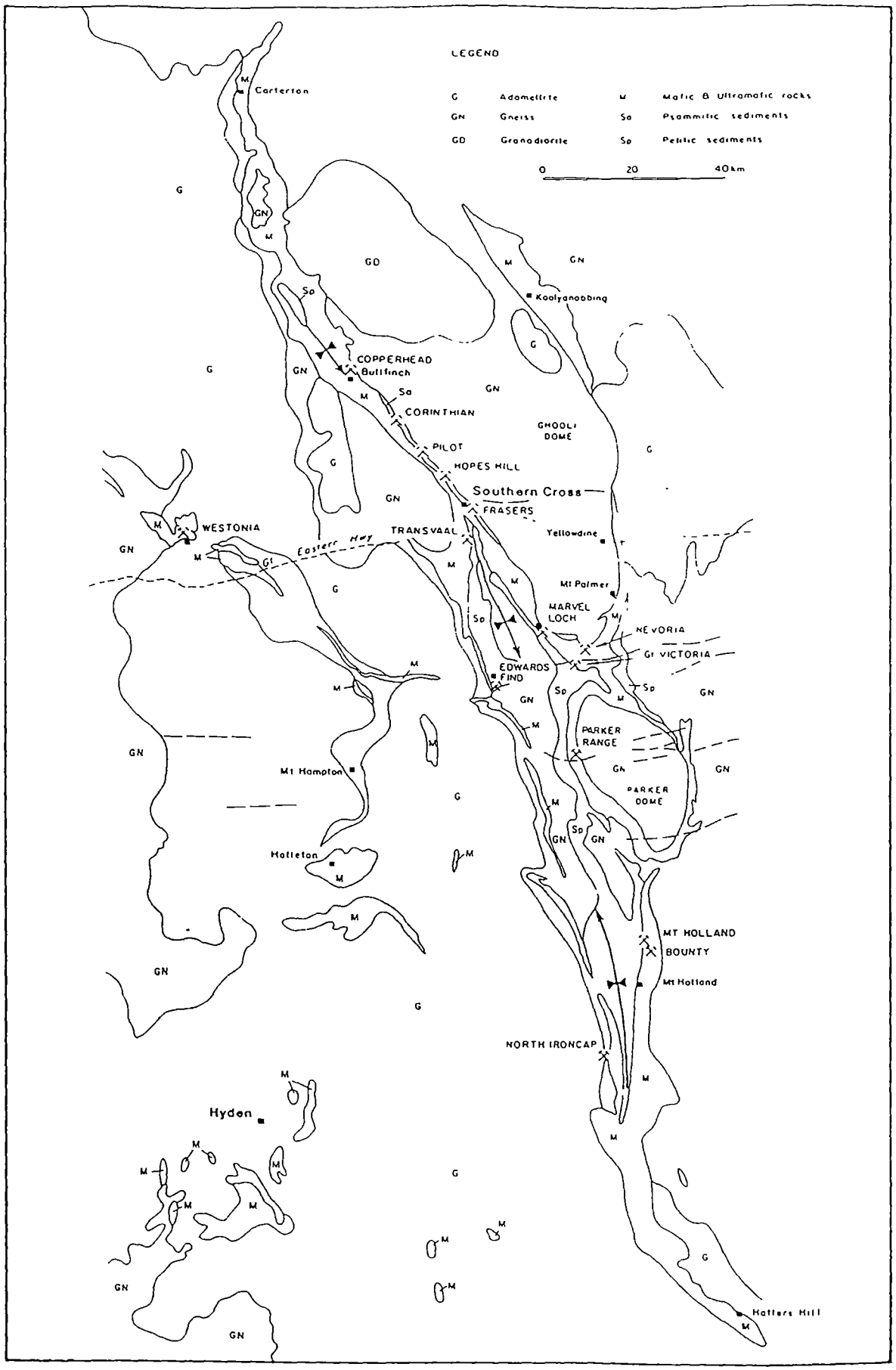

Figure 2: Regional geology and location of gold mines. Adapted from Aztec Mining Company Limited unpublished reports.

METHODOLOGY

In this study, a regional geological map and colour contoured aeromagnetic data are compiled to highlight the regional tectono-thermal history and geological setting of the Bounty deposit.

On the mine scale, rock types, fold styles and deformation fabrics were mapped from core through a typical cross-section of the deposit, section 34920N utilizing hole numbers MD02, MD12, MD24, MD41, MD44, MD71, MD71A and MD71B. Data was correlated with gold grade and modal sulphide content (visual estimate) and allied with detailed microstructural observations of selected samples. Orientations of bedding, folds, and deformation fabrics were measured from available oriented core (hole numbers MD77, MD78, MD79, MD84, MD85A, MD88 and MD88A) and some pit measurements. Few pit measurements were collected as structures of interest are generally associated within or adjacent to magnetic lithologies. Core structures were measured in their real orientations with assistance of an orientation jig.

Also in this study, the distribution of gold within the main mineralized structure is compared to changes in its form and orientation.

REGIONAL GEOLOGICAL SETTING

Regional geological mapping (Chin et al., 1984; Martyn, 1988) have shown the Forrestania Greenstone Belt as an asymmetric regional syncline with its axis interpreted to plunge gently north (Fig. 2). Outer limbs of mafic and ultramafic volcanic stratigraphy with intercalated iron formations and cherts are folded about a core of pelitic and psammitic sediments. Stratigraphy dips steeply (70-90°) west on the eastern limb and varies between 30° and 80° east on the western limb. Ultramafic volcanics associated with nickel sulfides occur on both limbs and inferred facing from their stratigraphy (Porter and McKay, 1981) suggests the synform is synclinal. A regional bedding parallel foliation formed during development of the syncline.

More recently, Davies (1990) and Rutherford (1991, this edition) have defined numerous broad ductile deformation zones (up to about 100m wide) which trend parallel to the axis of the interpreted syncline and are continuous over many tens of kilometres (Fig. 3, see page 74). The deformation zones occur subparallel to bedding, locally truncating it and some regional-scale upright fold structures (e.g. Mt Holland). They are characterized by a strongly developed foliation, down-dip elongation lineations with some thrust movement vectors reported (Davies, 1990). These structures, the complex upright fold structures and the dominant bedding parallel fabrics are interpreted to have developed during a regional period of strong east-west directed compression (Davies, 1990).

Massive batholiths, plutons and porphyritic stocks of granite-granodiorite composition, generally with a high magnetic susceptibility, intrude the syncline forming ovoid dome structures (Fig. 3 and Fig. 4, see pages 74 and 75 respectively). Similar granites occur along the margins of the Forrestania Greenstone Belt, defining its cuspate shaped boundary, and intrude along the major ductile deformation zones (Fig. 3). This suite of intrusives have deformed margins and are described by Davies (1990) as syntectonic with respect to the east-west directed compression.

Broad contact metamorphic aureoles up to medium-high grade (upper amphibolite facies) surround the syntectonic batholiths in the Southern Cross and Forrestania Greenstone Belts (Ahmat, 1986; Mueller, 1988). The broadness of the aureoles is the result of the relatively high ambient temperature of the greenstones at the time of emplacement (Mueller et al., 1991, Fig. 5). Regional metamorphism, probably synchronous with folding of the greenstone sequence, may have taken place at conditions of very low (prehnite-pumpellyite facies) to low metamorphic grade (greenschist facies – Mueller, 1988; Mueller et al., 1991).

East-northeast trending fracture zones cut across the greenstone belt and are intruded with Proterozoic dolerite and gabbro.

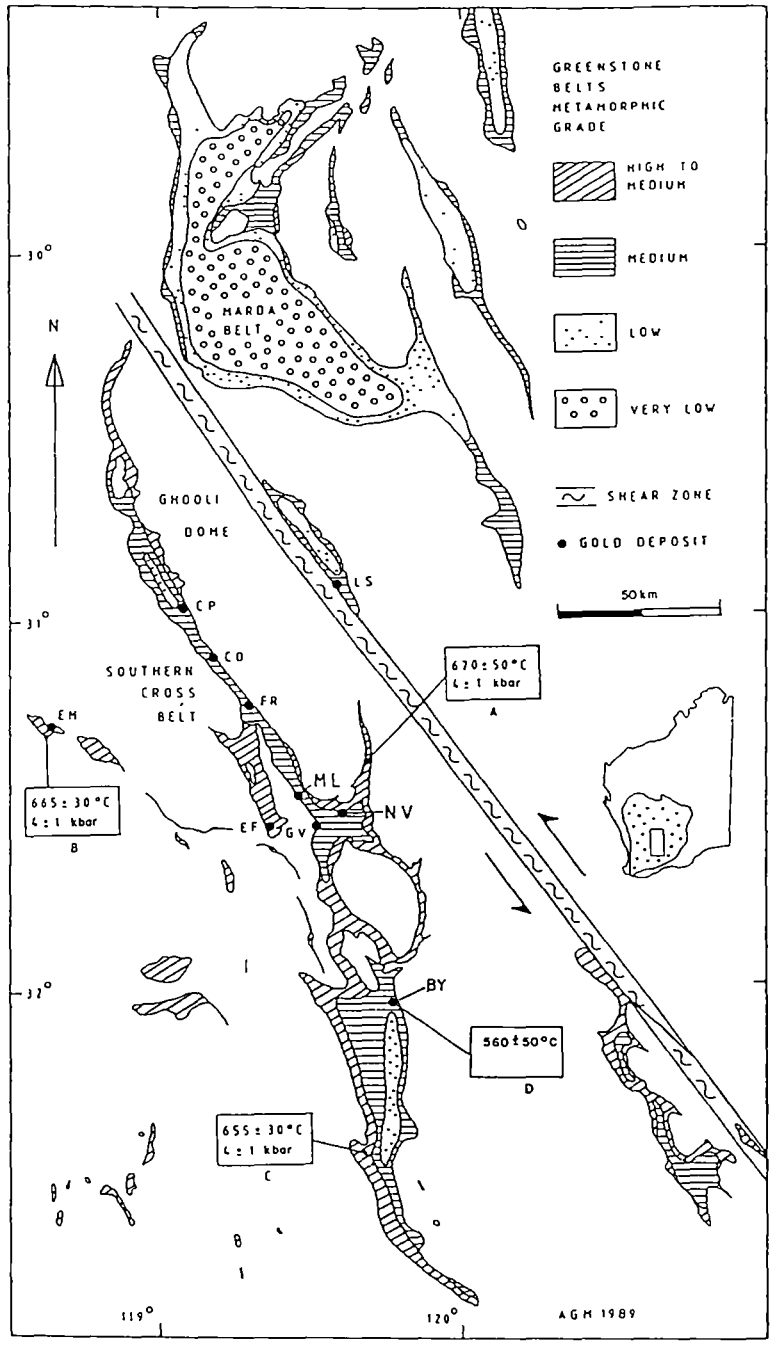

Figure 5: Generalized map of the Southern Cross area showing the distribution of metamorphic grade within the greenstone belt (modified from Mueller et al., 1991; after Ahmat, 1986) relative to the contacts of the granitoid batholiths (e.g. Ghooli Dome). Metamorphic nomenclature follows Winkler (1979). The metamorphic P–T data are from (A) Gole and Klein (1981); (B) Blight and Barley (1981) and Ahmat (1986); (C) Porter and McKay (1981); (D) Caswell (1989). Granodiorite–hosted Aw–Mo–W deposits: Edna May (EM). Greenstone–hosted gold skarn deposits: Corinthian (CO), Copperhead (CP), Edward's Find (EF), Fraser's (FR), Great Victoria (GV), Lake Seabrook (LS), Marvel Loch (ML), Nevoria (NV). Greenstone–hosted skarn–like gold deposit: Bounty (BY). The inset map of Western Australia shows the location of the Southern Cross area in the Yilgarn Block.

MINE GEOLOGY AND STRUCTURE

LOCAL GEOLOGICAL SETTING

Stratigraphy

The Bounty gold deposit is located within greenstones on the eastern limb of the interpreted regional syncline which dip between 70° and 90° west.

Oldest greenstone rocks occur along the eastern margin of the greenstone belt and consist of a thick pile of iron tholeiitic basalts and dolerites with minor high-Mg basalt flows and exhalitive sediment horizons (Fig. 3). This sequence forms the stratigraphic footwall to a predominantly ultramafic volcanic sequence referred to as the Bounty Sequence (Davies, 1990).

The Bounty Sequence is about 600m thick and has been mapped from an area south of Parker Dome south to Hatters Hill (Fig. 2 and Fig. 3). Volcanic rocks within the Bounty Sequence include komatiitic peridotites, komatiitic basalts and rare high-Mg basalts. Numerous intercalated cherts, iron formations and pelites of variable thickness and lateral continuity are also present. Gross stratigraphic cyclicity of the ultramafic sequence (basal komatiitic peridotite with nickel-bearing sulfides through komatiitic basalts, high-magnesium basalts overlain by exhalitive sediment) indicate a westerly younging direction (Porter and McKay, 1981; Martyn, 1988).

Overlying the Bounty Sequence is a thick pile of high-Mg basalts and komatiitic basalts (Fig. 3). Volcanics exhibit gabbroic textures, variolitic textures, spinifex textures and pillow structures. Exhalative sediment horizons of variable strike length are a minor component.

Pelitic and psammitic sediments with intercalated horizons of iron formation occur within the regional synclinal axis and represent the youngest greenstone stratigraphy (Fig. 3).

Tectono-Thermal History

During the period of strong east-west directed compression (Davies, 1990) a bedding parallel foliation, upright, gently plunging folds and regional-scale ductile deformation zones and thrusts developed in the area. With cessation or relaxation of the compression, syntectonic plutons with broad contact metamorphic aureoles and high magnetic susceptibilities were intruded. They occur along the eastern margin of the belt, dome sediments located within the central core and intrude as stocks and dykes along the regional ductile deformation zones (Fig. 3 and Fig. 4). Bounty Sequence in the vicinity of the Bounty Mine was rotated west of north during and as the result of emplacement of a syntectonic pluton (Fig. 3 and Fig. 4). The porphyritic stocks and dykes, and regional plutons in the area have deformed margins indicating that they were affected by strain which post-dated the regional east-west directed compression.

Mineral assemblages from basic rocks southwest and southeast of the Bounty deposit reflect a peak contact metamorphic grade of transitional amphibolite to lower amphibolite facies. These assemblages are hornblende - plagioclase and actinolite - plagioclase - epidote (minor) respectively (Turner, 1981). Also characteristic of amphibolite facies are iron formation assemblages of grunerite - quartz - magnetite in the Bounty Sequence, pelitic assemblages of biotite - garnet occurring within the Bounty Horizon, south of the deposit, and andalusite - biotite - white mica within the central core of sediments (Binns et al., 1976; Ahmat, 1984). Geothermometry on biotite - garnet assemblages from pelitic beds in the Bounty Horizon, located within the deposit gave a peak metamorphic temperature of 560°C ± 50°C (Caswell, 1989; Fig. 5).

Regional fracture zones and faults, with retrograde mineral assemblages trend in a northwest direction. They occur over lengths of about 1-5 kilometres with some continuous from the greenstones across the boundary with the syntectonic plutons.

Graphic textured granites and pegmatites containing muscovite or biotite intrude as flat dipping sheets or vertical dykes along the regional ductile deformation zones, the northwest trending faults and other crustal weaknesses (Fig. 3). Schorl-rich, spodumene-rich and muscovite-rich pegmatites are observed. Rare rubellite-rich varieties have been mined (Camp No Name rubellite prospect). East-northeast trending fracture zones intruded by Proterozoic dolerite and gabbro cut across the pegmatites and the greenstone belt (Fig. 3 and Fig. 4).

MINE SEQUENCE GEOLOGY

The Bounty orebody is stratabound within a sheared iron formation referred to as the Bounty Horizon which dips steeply west. The Bounty Horizon marks the top of the Bounty Sequence and is the westernmost exhalitive sediment horizon. Footwall komatiite peridotites and komatiite basalts of the Bounty Sequence and a hanging wall gabbro bound the mineralized Horizon (Fig. 3 and Fig. 6, see pages 74 and 76 respectively).

Porphyritic intrusives, graphic textured pegmatites and Proterozoic dykes intrude the ore environment (see section on intrusives). A Proterozoic dyke, referred to as the Binneringie Dyke, cuts across the Bounty deposit. The dyke is about 250 metres wide, subvertically dipping and separates the Main Bounty lode from the smaller North Bounty lode (Fig. 3). Archaean stratigraphy is continuous across the dyke.

Footwall Komatiitic Volcanics

Footwall komatiitic volcanic rocks adjacent the Bounty Horizon vary in composition from basaltic to peridotitic. Komatiitic basalts may be foliated, but generally comprise medium-grained, pale-green coloured actinolite ± biotite with an acicular, radiating texture. Plagioclase abundance is variable but generally minor. Komatiitic peridotites are fine-grained to medium-grained amphibole – serpentine – magnetite ± chlorite ± talc rocks. Spinifex textures are common throughout with blades varying from about 2cm up to 30cm long.

Bounty Horizon

Bounty Horizon within the mine area is a sheared amphibole–iron formation varying from about 15 metres to 30 metres thick. It is vertically and laterally continuous and dips between about 70° and 90° towards about 265° to 280°. The intensity of deformation within the horizon is variable, ranging from weakly deformed where primary bedding characteristics are preserved, to strongly deformed and mylonitic where primary bedding is destroyed (Fig. 6, see page 76). Spatial variation in strain through the Bounty Horizon is discussed in the section on structure.

Zones of low strain preserve planar bedding (So), defined by alternating iron–rich beds (50%) and chert–rich beds (50%). Thickness of bedding varies from 0.4mm up to 150mm but is generally about 10 to 50mm.

Iron–rich beds consist predominantly of grunerite ± ferro–actinolite, magnetite – biotite, magnetite – grunerite ± ferro–actinolite, or magnetite – plagioclase (rare) assemblages. Thin, iron–rich pelitic interbeds are less common and contain assemblages of biotite – garnet ± hornblende ± quartz. Chert–rich beds comprise granoblastic quartz with some magnetite, grunerite ± ferro–actinolite (Fig. 7 and Fig. 8).

Dominant amphiboles within weakly deformed, weakly mineralized, Bounty Horizon include grunerite (60–80%) and ferro–actinolite (20–40%). Grunerite is partially replaced by ferro–actinolite (Caswell, 1989).

Textures indicate recrystallization of iron formation assemblages (Fig. 9 and Fig. 10). Millimetre–scale grains of euhedral magnetite with a central inclusion of pyrrhotite occur as cores to acicular, radiating grunerite clusters which develop in a mass of granoblastic quartz. Here also, hedenbergite occurs as bedding parallel bands and crosscutting bands (possible veins) with corroded margins and inclusions of grunerite. Grunerite appears to replace hedenbergite during recrystallization. Magnetite recrystallization appears to post–date sulfidation.

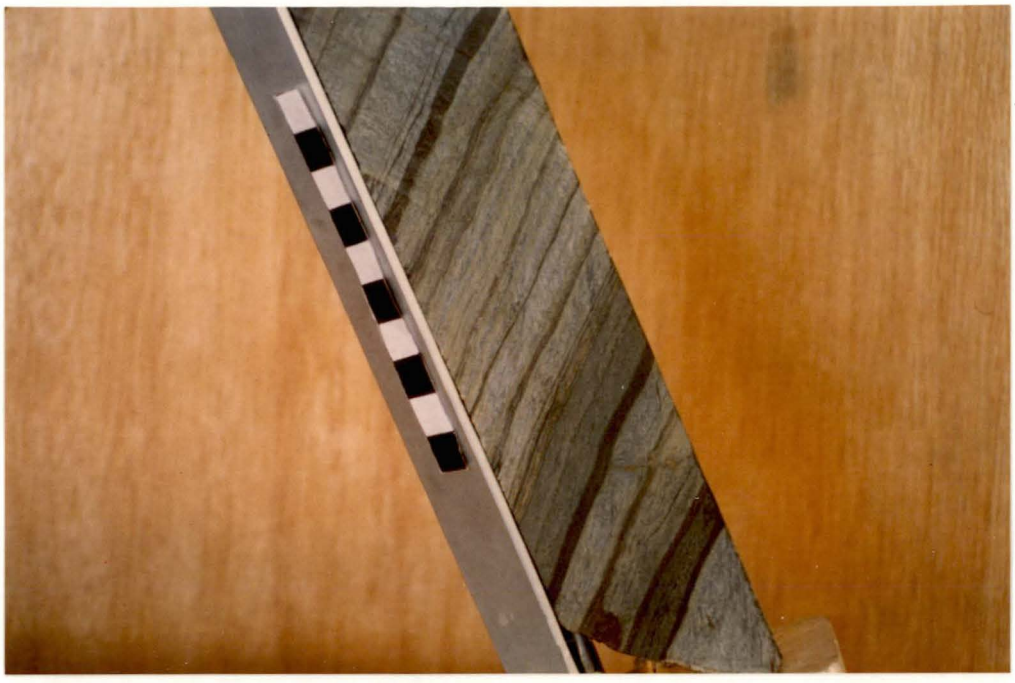

Figure 7. Weakly deformed Bounty Horizon viewed in real orientation facing north. Alternating chert–rich and iron–rich beds (So). Note steep, westerly dip angle (scale bar in centimetres, MD24, 199.3m)

Figure 8. Photomicrograph of weakly deformed Bounty Horizon viewed in real orientation facing north. Grunerite – magnetite – actinolite, magnetite – biotite, grunerite – actinolite and quartz – grunerite – actinolite – magnetite beds. Note ferro–actinolite replacing grunerite (318024, photo length = 6.7mm, ppl)

Figure 9. Weakly deformed, recrystallized bedding viewed in real orientation facing south. Note coarse grained magnetite (scale bar in centimetres, MD44, 354.25m)

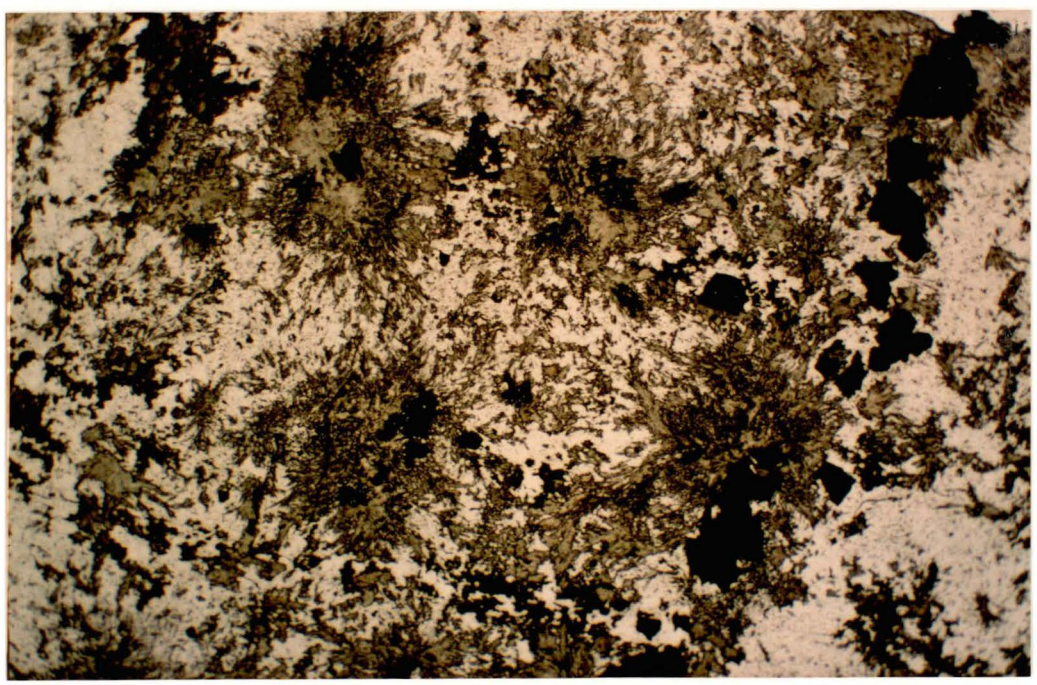

Figure 10. Photomicrograph of weakly deformed, recrystallized bedding showing acicular, radiating grunerite clusters surrounding coarse grained euhedral magnetites with central cores of pyrrhotite. Polygonal granoblastic quartz (318033, photo length = 13.5mm, ppl)

Hanging Wall Gabbro

The hanging wall gabbro is fine-grained to coarse-grained with a granular, decussate texture of subhedral hornblende after pyroxene (40-60%), plagioclase (40-60%), some actinolite, and variable amounts of biotite (Fig. 11). The gabbro appears to be homogeneous, although minor pyroxenitic layers and rare tremolite-rich layers occur towards the lower contact with the Bounty Horizon. A chilled margin is present adjacent to the lower contact, which is sheared. Contact with overlying komatiitic basalts is texturally gradational.

MINE SEQUENCE STRUCTURE

Introduction

Deformation within the Bounty deposit is dominated by simple shearing (Dn). The development of strain partitioning during shearing has resulted in mappable structural zones within and adjacent to the Bounty Horizon (Fig. 6, Appendix II). Shearing developed foliation surfaces (Sn) oriented subparallel to So, down-dip elongation lineations (Ln) and asymmetric fold structures (Fn) and fabrics (Appendix I). A zone of highest strain occurs within Bounty Horizon adjacent to the hanging wall gabbro (hanging wall shear zone). A second zone occurs within footwall rocks adjacent to or locally in the Bounty Horizon (footwall shear zone). The Bounty shear zones locally transgress the major lithological boundaries, but are generally parallel to the gross stratigraphy. They appear to continue northwards beyond the deposit but are suspected, from core and mine observations, to thin and horse tail towards the south. The following section describes geological characteristics of structural zones within the Bounty deposit and the nature and timing of veins and intrusives with respect to shearing (Dn).

Figure 11. Massive hornblende – plagioclase gabbro viewed in real orientation facing north (MD24, 179m)

Footwall Komatiitic Volcanics

Most exposures of footwall rocks preserve a weak Sn overprinted by random oriented actinolite growth. Strain appears to have been partitioned throughout the volcanic sequence and is greatest adjacent to the Bounty Horizon (footwall shear zone). Sn is mainly defined by alignment of actinolite ± biotite in komatiitic basalts and amphibole – chlorite ± talc in komatiitic peridotites. Elongate quartz – pyrite ± actinolite veins define a rarely observed elongation lineation (Fig. 12). This, and a paralleling actinolite mineral lineation (Ln) plunge 85° towards 274° (Fig. 13).

Veins

A zone of intense veining occurs within footwall rocks adjacent to the Bounty Horizon (Fig. 14). The zone varies in thickness from one to several metres with veins constituting 50% of the rock. Veins are oriented parallel to Sn and are about 10–100mm long, 3–10mm wide. Both deformed (early–Dn) and undeformed (post–Dn) veins are recognized (Fig. 6).

Deformed veins comprise quartz – pyrite ± actinolite ± pyrrhotite? in variable proportions. Vein minerals are either strongly deformed or recrystallized with a polygonal, granoblastic texture. Adjacent to the Bounty Horizon the veins have been folded during Dn and are locally transposed. Folds are asymmetric or intra–folial and gently plunging to the south. The foliation defined by actinolite, as described above, is axial planar to the folded veins. A similar deformed vein zone occurs in the footwall about 40m east of the Bounty Horizon (MD79, 344.87–359.0 metres).

The undeformed veins are parallel to Sn but overprint the fabric and have irregular shaped margins. As such, they are described as post–Dn. They comprise coarse grained clinopyroxene (3–10mm) with inclusions of calcite, euhedral epidote and an outer rim of clinozoisite (Fig. 15). Some vein quartz is present. Actinolite appears to be recrystallized adjacent to the vein margins.

Figure 12. Photomicrograph of elongate quartz – pyrite ± actinolite veins in sheared footwall komatiitic basalt. Viewed normal to Sn. Note down–dip elongation lineation defined by the vein and extensional pull apart structures with subhorizontal plunging necks (318036, photo length = 13.5mm, ppl)

Figure 13. Photomicrograph of actinolite mineral lineation (Ln) in sheared footwall komatiitic basalts. Viewed normal to Sn. Note recrystallized quartz – pyrite vein on left and actinolite porphyroblasts cutting across Ln and Sn (318023, photo length = 6.7mm, xpl)

Figure 14. Veined footwall komatiitic basalt viewed in real orientation facing south. Note the white coloured, transposed and folded quartz – pyrite ± actinolite veins (early–Dn) and the undeformed, pale–green coloured calcsilicate – calcite – quartz veins with irregular shaped margins (post–Dn; MD71B, 534m)

Figure 15. Photomicrograph of post–Dn calcsilicate – calcite – quartz vein overprinting Sn in footwall komatiitic basalts. Vein consists of coarse grained clinopyroxene with inclusions of epidote and calcite and an outer rim of clinozoisite, actinolite and quartz (318026, photo length = 3.5mm, ppl)

Weakly Deformed Bounty Horizon

Bounty Horizon of the weakly deformed category is poorly mineralized and preserves primary bedding (So) characteristics as described in the previous section. Less well recrystallized bedding preserves a weak bedding parallel foliation (Sn) defined by elongate clusters of magnetite with polygonal grain boundaries.

Veins

Rare veins containing hedenbergite – quartz – calcite – garnet – apatite assemblages occur parallel to bedding (Fig. 6, Fig. 16 and Fig. 17). Quartz within these veins preserve a strong foliation parallel to bedding (Sn) which wraps around coarse-grained hedenbergite. As such, the veins are described as early with respect to Dn (shearing).

Moderately Deformed Bounty Horizon

The boundary between the weakly deformed zone and this zone is either gradational or sharp. Moderately deformed Bounty Horizon is characterized by asymmetrically folded bedding (Fn), pyrrhotite-matrix breccias and spaced zones of strong foliation (Sn) and discontinuous So (Fig. 6 and Fig. 18).

A sharp contact is generally defined by the presence of a pyrrhotite-matrix breccia subparallel to bedding (Fig. 6 and Fig. 18). These breccias vary in thickness from about 2cm up to 200cm and comprise clasts of deformed iron formation (some rotated) or calc-silicate, quartz or calcite minerals floating in a matrix of pyrrhotite (Fig. 19 and Fig. 20). Where a breccia zone is not observed, transition from the weakly deformed to moderately deformed is gradational. The moderately deformed zone is recognizable by tighter, more frequently formed folds, zones more pronounced foliation, and a greater gold grade and sulphide content (Fig. 6).

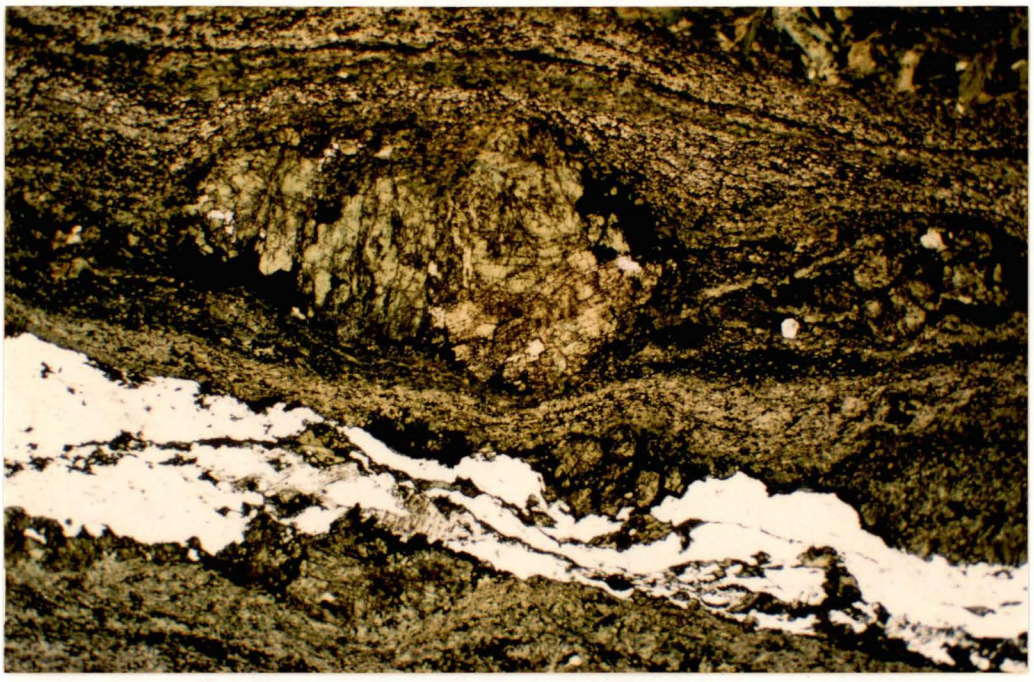

Figure 16. Photomicrograph of quartz – hedenbergite – calcite – garnet – apatite vein which has been deformed during Dn. Quartz has a mylonitic fabric (Sn) parallel to So. Hedenbergite selvage (centre) is recrystallized to grunerite. Grunerite and possibly hedenbergite are replaced by ferro–actinolite. Dn pressure shadow around hedenbergite augen. Fractures in quartz, grunerite, hedenbergite and ferro–actinolite are filled with pyrrhotite. Note euhedral apatite crystal (white) in hedenbergite selvage (318019, photo length = 13.5mm, ppl)

Figure 17. Photomicrograph of hedenbergite augen (from Fig. 15) partially recrystallized to grunerite (white). Grunerite appears to have been replaced by ferro–actinolite (dark green) (318019, photo length = 1.3mm, ppl)

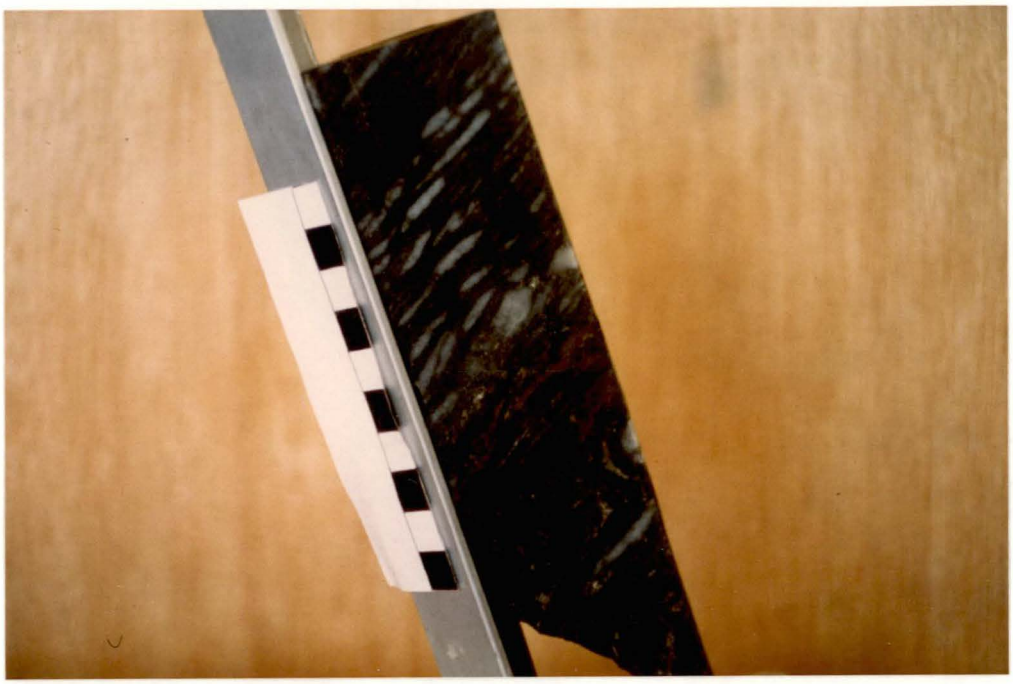

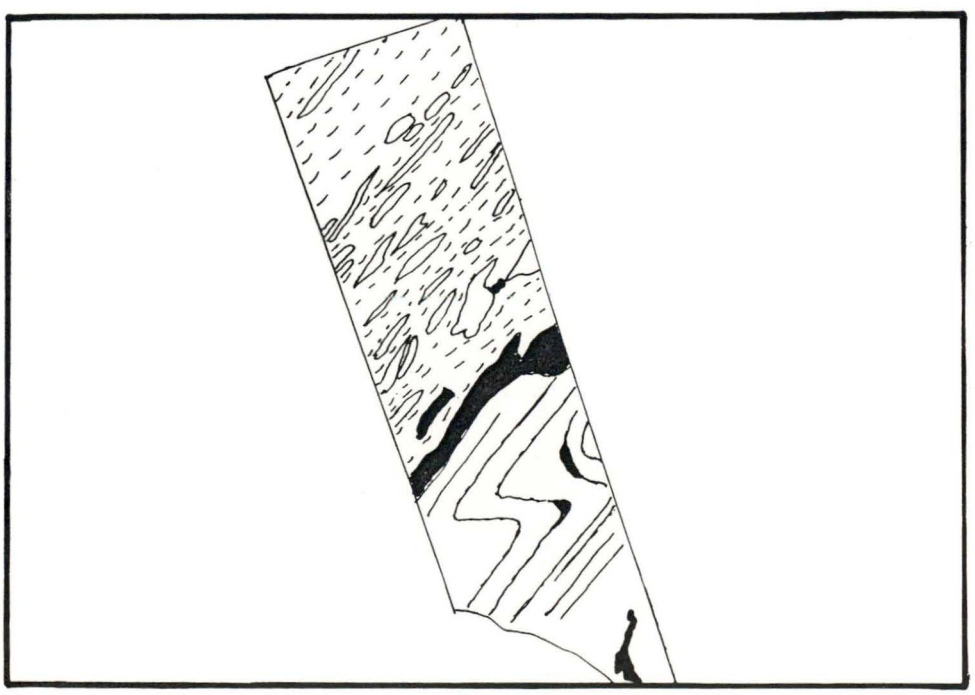

Figure 18. Typical relationship between Dn folded bedding (solid line), pyrrhotite-matrix breccias (black) and spaced zones of strong foliation (dashed line) seen in the moderately deformed zone of Bounty Horizon. Specimen viewed in real orientation facing north. Note asymmetry of Fn structure and the development of pyrrhotite in Fn hinge zones and along the boundary between folded bedding and a strongly deformed and foliated zone (scale bar in centimetres, MD71, 608.6m)

Figure 19. Pyrrhotite–matrix breccia viewed in real orientation facing north. Gold–poor, with clasts of quartz, actinolite and deformed iron formation comprising quartz – actinolite – biotite ± clinozoisite (scale bar in centimetres, MD44, 348.5m)

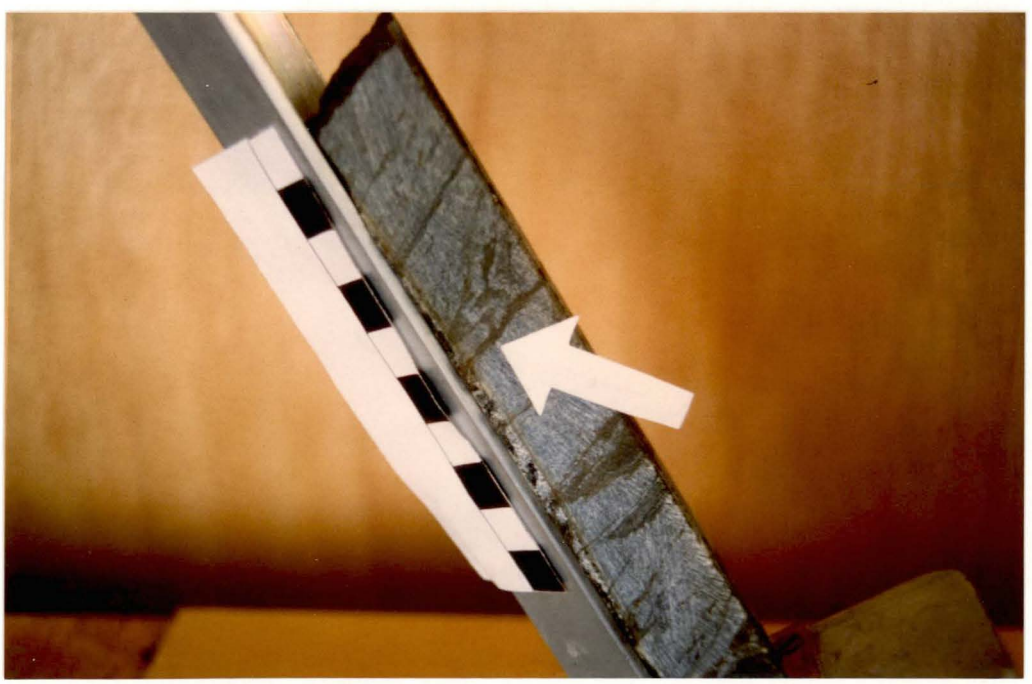

Figure 20. Moderately deformed zone viewed in real orientation facing south. Transposed fold structure with pyrrhotite–matrix breccia developed along the transposing shear surface (white arrow). Note shear surface is axial planar to Fn (scale bar in centimetres, MD2, 94.6m)

Fn Structures

Fn structures have an upright, asymmetric shape with predominantly gentle south-southeast and north-northwest plunging axes (Fig. 18, Fig. 20, Fig. 21, Fig. 22 and Appendix I). Fold closures in the Moderately Deformed Bounty Horizon vary progressively from open to tight near the weakly deformed zone, to tight or isoclinal towards the strongly deformed zone (Fig. 6). A fanning foliation (Sn) develops in fold hinge areas and fold amplitudes vary from metre-scales to millimetre scales.

The predominant fold asymmetry for folds with their long limb (So) dipping west is consistent with formation during west-down, normal movement along a shear surface parallel to So (Fig. 6 and Fig. 18). Most open to tight folds measured in the moderately deformed zone plunge about 18° towards 193°, although some do plunge about 13° towards 351° (Fig. 23). Axial planes to folds with west-down, normal profiles strike north-south and dip 55° west (Fig. 23A), but steepen as the strongly deformed zone is approached (Fig. 23B).

Fold profiles with an opposite asymmetry are less common and appear to be only observed where So dips near vertically or towards the east. Here the asymmetry is consistent with formation during east-down, normal movement along a shear surface parallel to So. Axial planes to folds with east-down profiles are tentatively calculated to dip 76° towards 085° (Fig. 24).

The orientation of axial planes to open folds within the moderately deformed zone is consistent with normal shear movement along the west-dipping hanging wall shear zone (Fig. 23 and Fig. 24). From these observations, the maximum principle stress during Dn is estimated to be subvertical.

Figure 21. Photomicrograph of asymmetric crenulations (Fn) in west dipping biotite schist. Note biotite foliation and hornblende porphyroblasts are pre-Fn. Pyrrhotite located in Fn hinge zone. View facing north (318029, photo length = 6.7mm, ppl)

Figure 22. Photomicrograph of transposed asymmetric microfold (Fn) in west dipping bedding. View facing north. Note the zoned garnets and the microfaults normal and slightly oblique to So (east side) are infilled with pyrrhotite (318011, photo length = 13.5mm, ppl)

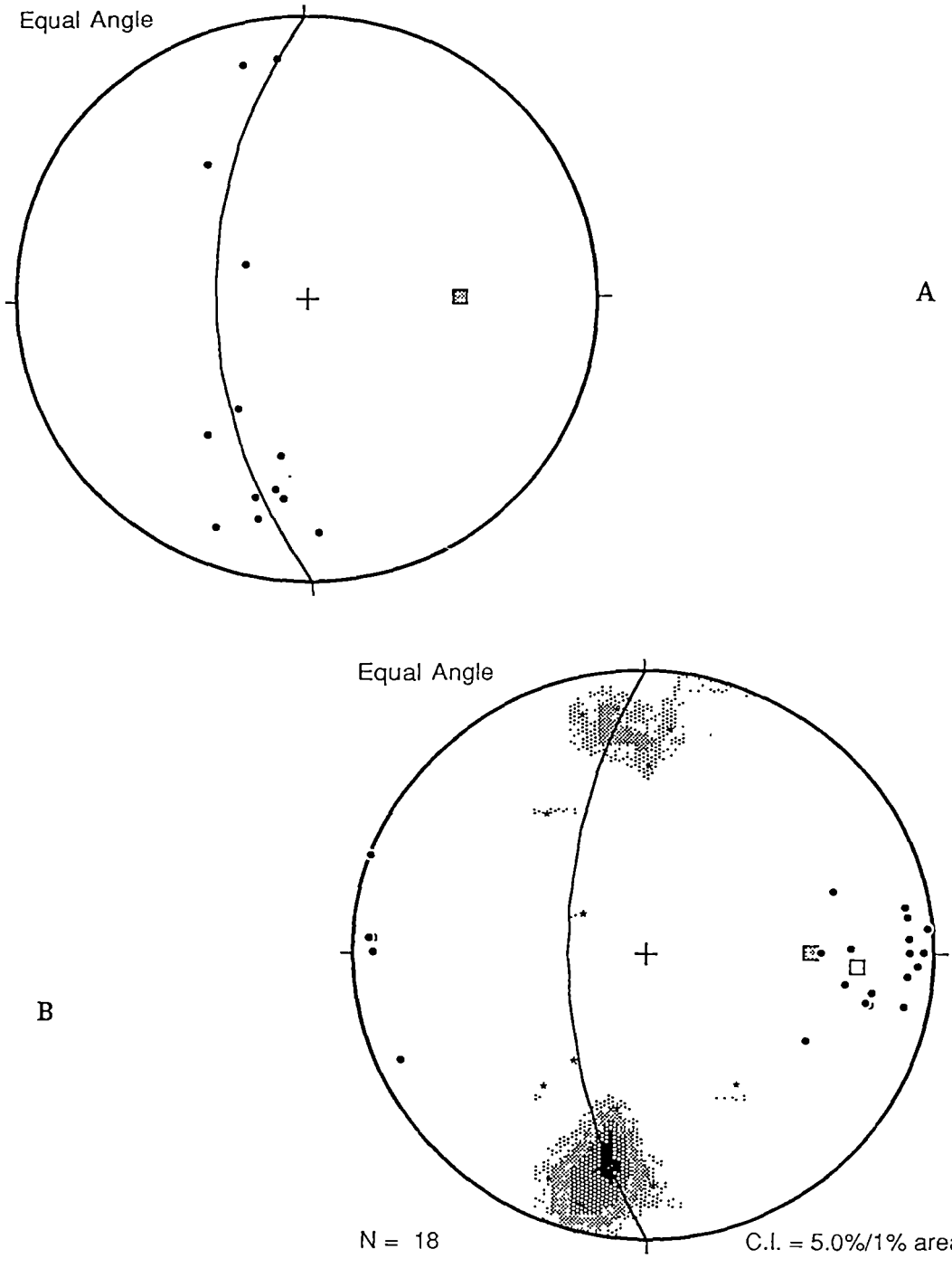

Figure 23 A. Equal angle stereographic projection of fold axes to asymmetric Fn structures with west-down normal profiles measured in the moderately deformed zone of the Bounty Horizon. Great circle equivalent to the axial plane of the Fn structures which dips 55° west

B. Equal angle stereographic projection of Fn fold axes as above (stars with shaded contours), and poles to Sn measured from strongly deformed zones of the Bounty Horizon (dots). Note that the pole to the axial plane of the Fn structures (shaded box) has a shallower dip than the average pole to Sn (white box). This is expected for folds with west-down, normal profiles (see text)

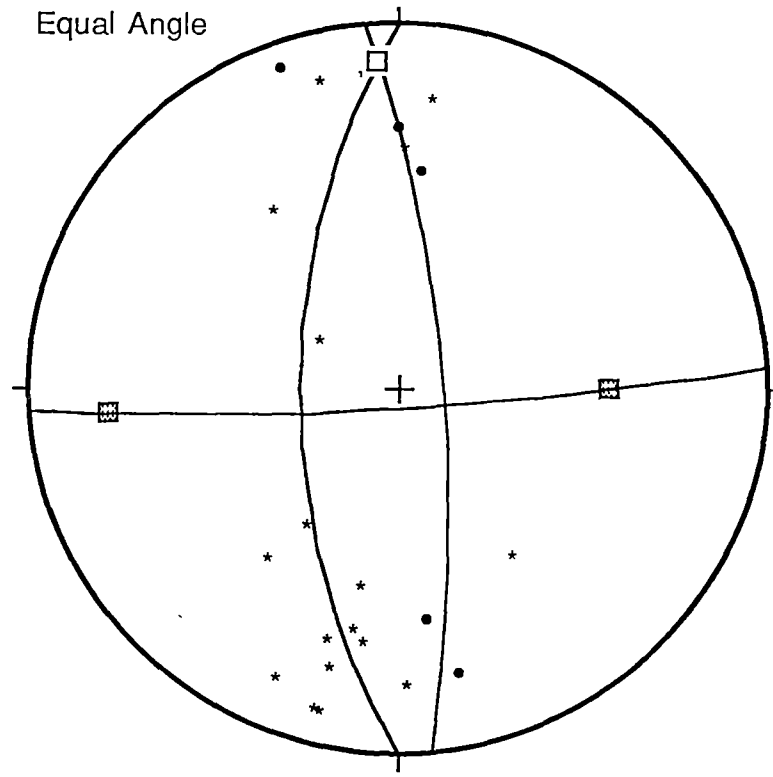

Figure 24. Equal angle stereographic projection of fold axes to Fn structures with west-down normal profiles (stars) and the less common east-down normal profiles (dots). Great circles and poles to the great circles define the orientation of their axial planes

Foliation

Discrete zones of strong foliation (Sn) up to about one metre wide have developed parallel to So and dip on average 83° towards 274° (Fig. 6, Fig. 23 and Appendix I). They are separated by zones of tightly folded iron formation, in which one or both limbs of tight, Fn structures are often transposed. Banding (once bedding) within the zones is parallel to the foliation, thin (0.4mm to 10mm), and discontinuous. Sulphide mineralization is most abundant in these zones.

Foliation throughout the moderately deformed iron formation is axial planar to tight Fn structures. The foliation is defined primarily by ribbon quartz or biotite in the more pelitic beds. Hedenbergite augens and magnetite clusters are also flattened and elongate and display tensional fractures normal to their elongation direction (Fig. 25 and Fig. 26). Amphiboles occur both parallel and overgrow the deformation fabric and are rarely preserved as a strong foliation. Garnet and hornblende porphyroblasts are wrapped by Sn developing asymmetric pressure shadows (Fig. 27 and Fig. 28).

Boudinage, Tension Fractures and Micro-Faults

Boudinaged beds with gently south plunging neck regions and tensional fractures oriented normal to So and Sn are common throughout the moderately deformed zone (Fig. 29). Micro-faults showing centimetre-scale offsets of chert beds occur parallel, or slightly oblique, to the foliation orientation (Fig. 22). Conjugate micro-faults have also been observed oriented near normal to the undeformed bedding orientation. Orientations of these structures, although not quantified, suggest they developed during a period of down dip elongation.

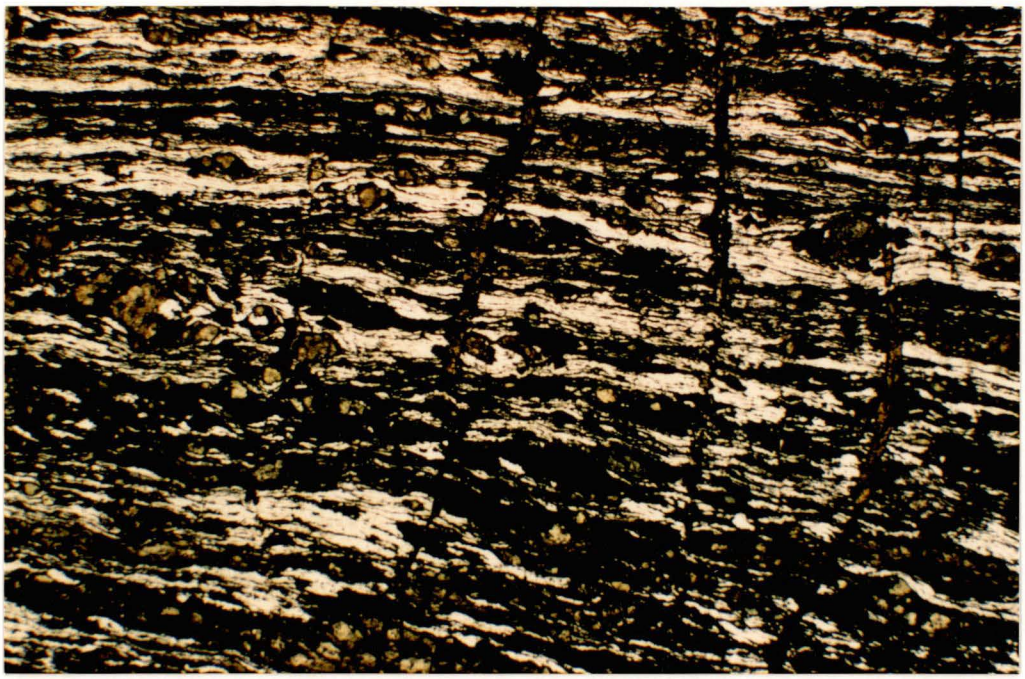

Figure 25. Photomicrograph of flattened and elongated hedenbergite and magnetite augens (Ln) in a matrix of ribbon quartz (Sn). Note pyrrhotite fills crosscutting veins oriented normal to Sn and Ln. Pyrrhotite replaces magnetite adjacent to these veins (318030, photo length = 6.7mm, ppl)

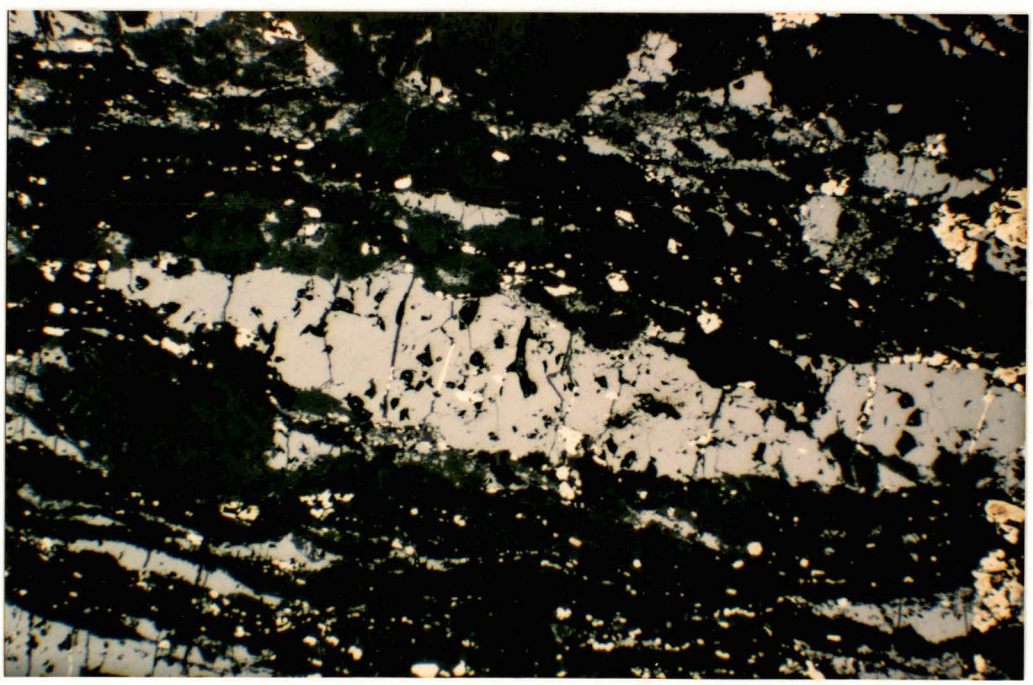

Figure 26. Photomicrograph of elongate magnetite augen (Ln) in Fig. 25 with tension fractures oriented normal to the elongation direction. Fractures infilled with pyrrhotite (318030, photo length = 1.3mm, reflected light)

Figure 27. Photomicrograph of deformed garnet and hornblende porphyroblasts with asymmetric pressure shadows filled with pyrrhotite (318031, photo length = 6.7mm, ppl)

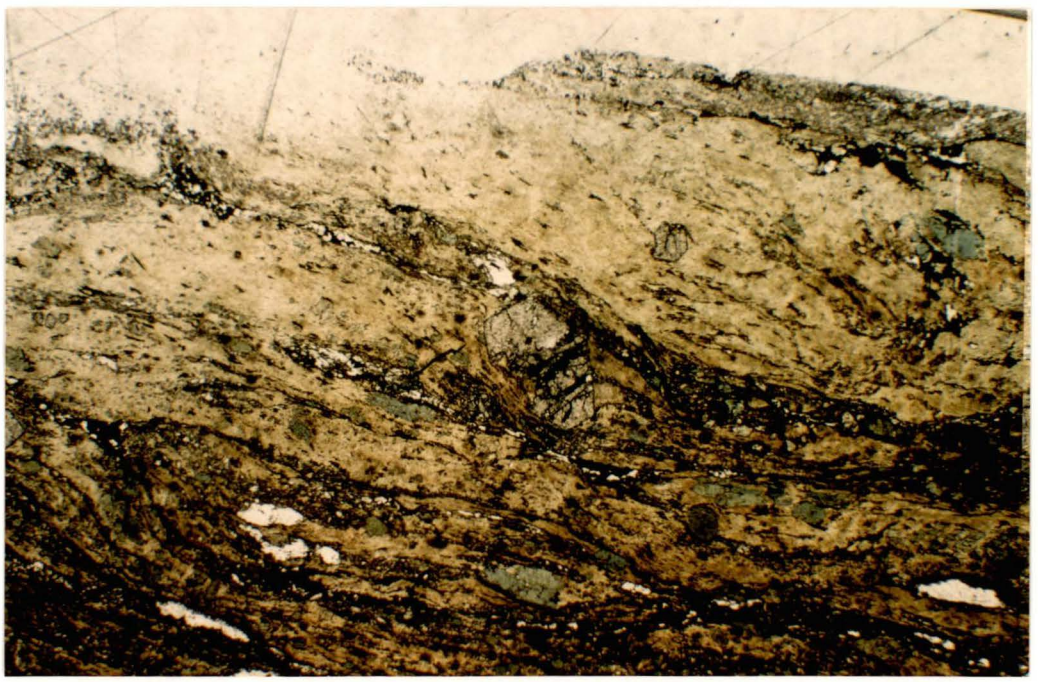

Figure 28. Photomicrograph of a flattened and pulled apart garnet porphyroblast (centre) oriented oblique to the shear fabric (Sn). Note tension fractures in garnet filled with pyrrhotite (318032, photo length = 6.7mm, ppl)

Figure 29. Tension vein infilled with pyrrhotite mineralization and developed normal to So. Indicates pyrrhotite was introduced during down-dip extension. Viewed in real orientation facing north (scale bar in centimetres, MD41, 240.2m)

Veins

Three main vein types are observed within moderately deformed zone. Early-Dn hedenbergite - quartz - apatite assemblages, syn-Dn to late-Dn pyrrhotite-rich veins and matrix breccias (with associated calc-silicate - calcite - quartz assemblages) and post-Dn calc-silicate - carbonate veins.

The early formed veins are deformed and define Sn and Fn structures. Pyrrhotite-rich veins and pyrrhotite-matrix breccias are developed parallel to Sn, in Fn hinge zones in boudin necks, and in tensional orientations and along microfaults oriented normal to Sn. Breccias also cut across mylonitic Sn and contain rotated clasts of the deformed iron formation (a more detailed description of the pyrrhotite mineralization is given in the section on mineralization). The post-Dn calc-silicate - carbonate veins cut across So and Sn, have irregular vein margins and a variable, coarse-grained mineral assemblage. Minerals include clinopyroxene, garnet, hornblende, epidote, clinozoisite, actinolite, calcite, ankerite, quartz with possible wollastonite(?) and tremolite(?).

F_{n+1} Structures

In the weak and moderately deformed zones, So and Sn appear to be buckle folded in localized zones (e.g. drive 4, 34920N to 34945N). Resulting folds (F_{n+1}) are steep plunging with vertical dipping axial planes striking in a northwesterly direction. Fold closures are open to tight with chevron and box shapes and have steep plunging axes.

Strongly Deformed Bounty Horizon

Strongly deformed zones of iron formation are developed subparallel to So, and occur adjacent to the hanging wall gabbro (hanging wall shear zone), and in some iron formation adjacent the footwall contact (footwall shear zone - see Appendix II,

Fig. 6). Both asymmetric and transposed structures and fabrics indicate that shearing dominated in these zones, which anastomose and locally transgress lithological boundaries. The hanging wall shear zone is about 2m to 7m wide, strongly mineralized and mainly developed in iron formation, rarely penetrating the gabbro (Fig. 6). The footwall shear zone is about 5m to 10m wide, and mainly developed in the komatiitic volcanic rocks. Deformed iron formation within, and marginal to, both shears appears similar, however, the footwall shear is generally gold-poor relative to the hanging wall shear. Exceptions of significant footwall mineralization do occur. The shears appear to converge within some parts of the iron formation (Appendix II).

Intense shearing, boudinage, folding and transposition in the strongly deformed zones resulted in a finely banded to laminated (0.4mm up to about 10mm) appearance of the rocks (Fig. 30 and Fig. 31). Strong bedding parallel foliation (Sn) is defined by minerals identical to those described defining foliation throughout the moderately deformed zone. S/C fabrics indicative of a normal sense of movement are observed (Fig. 32 and Fig. 33).

Sn is developed axial planar to gently plunging, transposed, asymmetric folds, rootless intrafolial folds, isoclinal folds (Fn) and, less common, steep plunging folds and sheath folds (Fig. 31). Fold closures vary progressively from tight towards the moderately deformed zone to isoclinal towards the chloritic contact shear (Fig. 6). Folds at centimetre and millimetre scales are most common. The predominant fold asymmetry is indicative of a normal sense of movement along a shear surface parallel to Sn.

Veins

Three vein styles are predominant within strongly deformed zones of the Bounty Horizon. Early-Dn quartz - calcite ± hedenbergite ± garnet veins, syn-Dn to late-Dn pyrrhotite-rich veins and matrix breccias, and late Dn-quartz ± visible gold veins.

Figure 30. Strongly deformed Bounty Horizon viewed in real orientation facing south. Note the discontinuous, transposed bedding. Contrast with Fig. 7 (scale bar in centimetres, MD71, 71.5m)

Figure 31. Photomicrograph of strongly deformed Bounty Horizon showing a transposed isoclinal fold (Fn) with its axial plane parallel to Sn. Sn defined by quartz, grunerite, actinolite and magnetite. Note magnetite – plagioclase bed in core of isocline. Pyrrhotite has replaced about 60% of the magnetite (318027, photo length = 13.5mm, ppl)

Figure 32. Photomicrograph of strongly deformed Bounty Horizon showing transposed quartz foliation (Sn) or possible S and C fabric (318027, photo length = 6.7mm, xpl)

Figure 33. Photomicrograph of the chloritic contact shear viewed in approximate real orientation facing north. S and C fabrics indicate normal (west–down) movement along shear surfaces (317681, photo length = 13.5mm, xpl)

The early formed veins are about 2cm up to 10cm wide, strongly fractured and foliated. The pyrrhotite-rich veins and breccias are identical to those described within the moderately deformed zone and make up about 50-60% of the strongly deformed zone. Pyrrhotite veins cut across the early formed veins.

Quartz ± visible gold veins are developed either subparallel or normal to Sn and So, cutting Fn structures. As such, they are described as late with respect to Dn. The veins are between 3cm and 20cm thick and continue along drives for about 1-10 metres. The veins occur throughout the Bounty Horizon but are most common in the strongly and moderately deformed zones.

Veins with visible gold comprise assemblages of quartz, calcite, hedenbergite with disseminated pyrrhotite ± pentlandite ± molybdenite ± chalcopyrite and selvages of hedenbergite - actinolite - calcite ± pyrrhotite ± visible gold (Fig. 34 and Fig. 35). Veins containing assemblages of quartz, actinolite, pyrrhotite, apatite and selvages of actinolite, biotite and clinozoisite do not contain visible gold (Fig. 34).

Chloritic Contact Shear

An anastomosing chloritic shear up to about 2m wide occurs at the contact between the hanging wall gabbro and the strongly deformed Bounty Horizon (Appendix I, Fig. 5). In outcrop it is visible as a smooth, shiny, black coloured surface (Fig. 36). The shear fabric is mylonitic and essentially defined by preferentially aligned, fine-grained chlorite after biotite, and elongate clasts and aggregates of deformed iron formation and quartz bands. Quartz aggregates within the shear are rod shaped with an apparent steep plunge, and have a granoblastic texture. S/C fabrics indicative of a normal sense of movement are observed (Fig. 33).

Figure 34. Photomicrograph of late–Dn veins of quartz ± visible gold. The central vein contains visible gold and consists of quartz, calcite, hedenbergite with disseminated pyrrhotite, pentlandite, molybdenite, chalcopyrite and selvages of hedenbergite, actinolite, pyrrhotite and visible gold. The vein on the right is free of visible gold and consists of quartz and actinolite with disseminated pyrrhotite and apatite and selvages of actinolite, biotite and clinozoisite (318614B, photo length = 13.5mm, ppl)

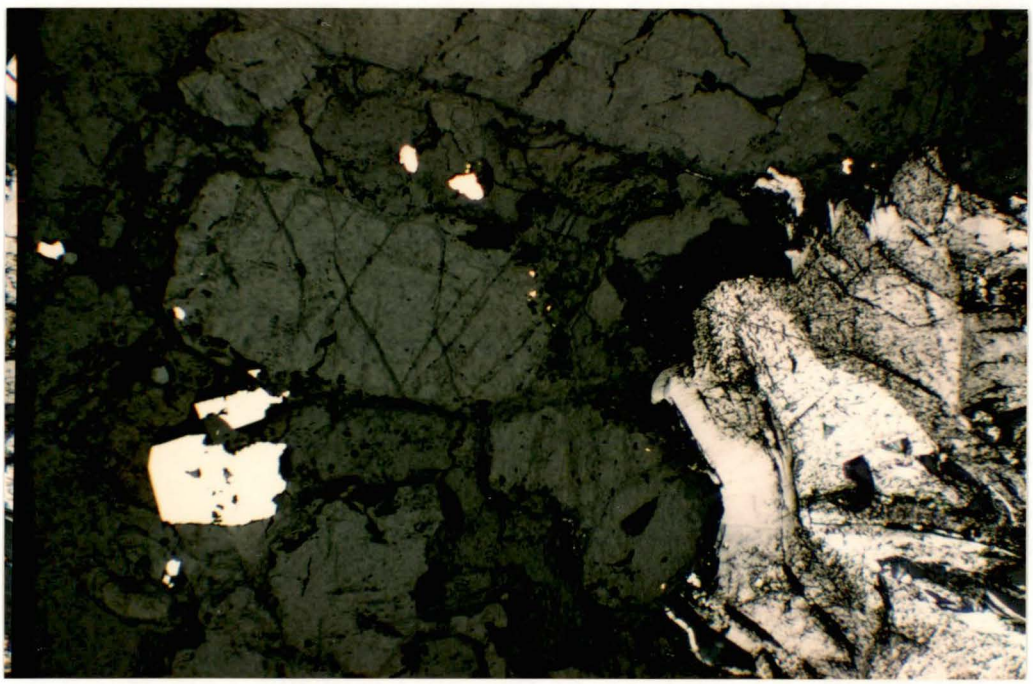

Figure 35. Photomicrograph of disseminated sulfide minerals in late-Dn quartz veins with visible gold. Molybdenite (right), pyrrhotite with lamallae of pentlandite (left) and gold in contact with pyrrhotite (centre) (318614B, photo length = 1.3mm, reflected light)

Figure 36. View in pit facing east of the chloritic contact shear. Note folds buckling the shear surface plunge gently towards the south

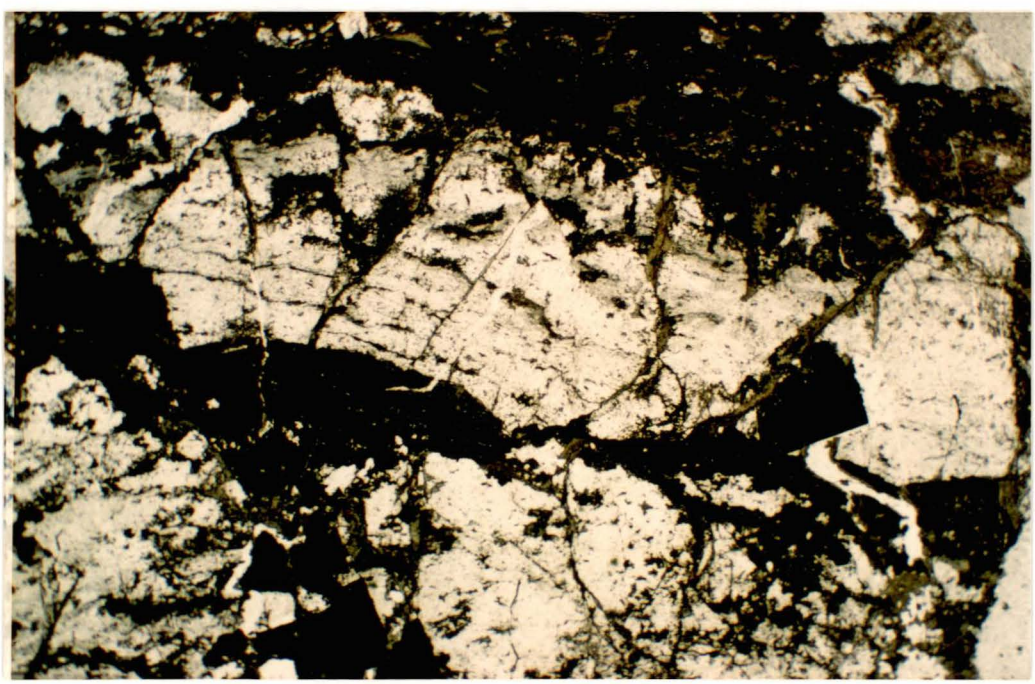

Figure 37. Photomicrograph of the chloritic contact shear. Chlorite replaces biotite and occurs in irregular oriented fractures cutting across the mylonitic quartz fabric and euhedral pyrites (317682B, photo length = 13.5mm, ppl)

Chlorite is ubiquitous and occurs replacing biotite along the foliation or in numerous crosscutting fractures (Fig. 37). Subhedral pyrite (1–2% visual estimate) and minor pyrrhotite within the shear is fractured and infilled with chlorite. Some graphite and carbonaceous material also occur within the shear, particularly towards the southern end of the deposit.

Veins

Folded and foliated veins of quartz – calcite ± garnet ± hedenbergite and undeformed quartz ± visible gold veins (as described in the strongly deformed zone) occur within the shear. The veins are generally oriented parallel to the boundaries of the shear.

Hanging Wall Gabbro

Strain within the gabbro is partitioned and localized along broadly spaced zones of foliation varying from about 0.5 to 3 metres wide. Foliation within the zones is moderately developed and defined by the alignment of biotite and hornblende, with biotite replacing most hornblende. The foliation parallels the contact with the Bounty Horizon (So) and as such is defined as Sn. Most of the gabbro is massive to only weakly foliated with biotite as a minor phase.

A second and younger deformation fabric (S_{n+1}), defined by subvertical zones of weakly developed fracture cleavage and veining is visible in the Bounty Pit (Fig. 38). This fabric strikes north–northwest and is defined by the preferred alignment of fractures intruded by subparallel quartz – epidote – chlorite ± calcite veins with chlorite alteration haloes (Fig. 38). S_{n+1} truncates Sn as defined by biotite, locally altering it to chlorite (Fig. 39).

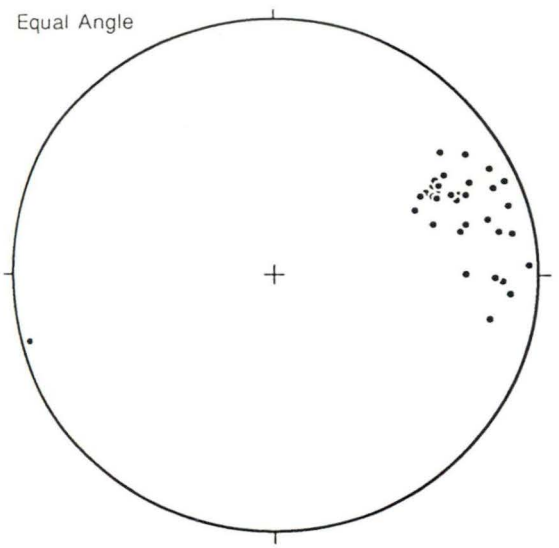

Figure 38. View in pit facing northwest of north-northwest trending fracture cleavage (S_{n+1}) intruded by quartz - epidote - chlorite veins with chlorite alteration haloes. Equal angle stereographic projection of poles to S_{n+1}

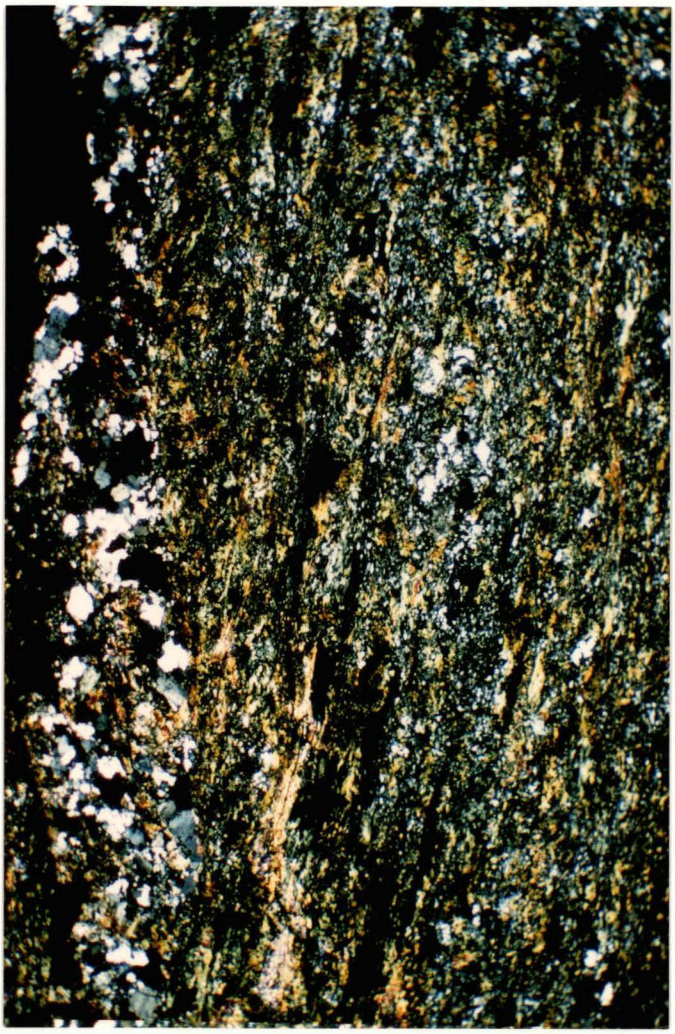

Figure 39. Photomicrograph of deformed hanging wall gabbro showing plan view of north–south trending biotite foliation (Sn) altered to chlorite (dark clots) adjacent to a north–northwest trending D_{n+1} quartz – epidote – chlorite vein (319693, photo length = 13.5mm, xpl)

Intrusives

Intrusive bodies within the Bounty deposit can be defined relative to Dn. Pre–Dn intrusives contain a weak to moderate foliation parallel to Sn and include quartz – feldspar porphyries and feldspar porphyries. A pre–Dn quartz – feldspar porphyry, visible in the pit, cuts across the hanging wall gabbro and terminates against the Hanging Wall Shear Zone where a strong foliation has developed parallel to the shear. Regionally, the porphyries are interpreted as the hypabyssal equivalents of the syntectonic porphyritic stocks and granitoid plutons and batholiths.

In the Bounty Mine, post–Dn shoal–rich pegmatites, spodumene–rich pegmatites, muscovite–rich pegmatites and the Proterozoic dyke suite occur as undeformed dykes or sills that truncate So, Sn and S_{n+1}. The pegmatites occur as subvertical sills or gently south–southeast dipping dykes and are truncated by east–northeast trending fracture zones along which the Proterozoic dykes intrude.

STRUCTURAL SYNTHESIS

Deformation in pre–Dn times was dominated by strong east–west compression, which resulted in complex upright folding and thrusting of the supracrustal sequence. Following this event, the deformed supracrustal sequence was intruded by granite–granodiorite plutons and porphyritic stocks, sill and dykes (Fig. 6).

Development of a vertical directed maximum compressive stress succeeded the intrusive event. Resulting strain (Dn) partitioned across the Bounty Sequence focused shear zones with a normal movement sense along the footwall and hanging wall boundaries of the Bounty Horizon. Strain partitioning produced a structural zonation within the Bounty Horizon. This is defined by three zones:

1. a weakly deformed zone where bedding characteristics are preserved;
2. a moderately deformed zone where bedding is folded and boundinaged; and
3. a strongly deformed zone where bedding is destroyed.

Normal movement along the shears developed asymmetric and transposed structures (Fn), bedding parallel fabrics (Sn), down dip elongation lineations (Ln), and extension structures normal to bedding. In the moderately deformed zone, gentle plunging asymmetric folds developed with open to tight closures and an axial planar foliation dipping 55° west. In higher strained zones, folds became isoclinal and transposed as their axial planes rotated into parallelism with the bedding–parallel shear planes.

As shearing progressed, mylonitic fabrics were overprinted by more brittle extensional structures oriented normal to the elongation direction.

A weak regional deformation event occurred after Dn. This event (D_{n+1}) is expressed as a north–northwest striking, subvertical fracture cleavage in the hanging wall gabbro, and as northwest trending fracture zones and faults on a regional scale. Quartz – epidote – chlorite ± calcite veins with chloritic alteration haloes occur along the fracture cleavage in the hanging wall gabbro and, as such, are interpreted as a D_{n+1} vein event. Buckle folds within the Bounty Horizon with a steep plunge and north–northwest trending axial planes are interpreted as F_{n+1} structures. Chloritisation of the sheared hanging wall boundary is interpreted to have occurred during this event.

Graphic textured granites and pegmatites intrude as flat dipping sheets or vertical dykes along the early thrusts, Dn shear zones, northwest trending regional faults and other crustal weaknesses. The pegmatites and earlier formed structures are cut across by east–northeast trending fracture zones along which Proterozoic dykes intrude.

MINERALIZATION AND ITS RELATIONSHIP TO DEFORMATION

Gold mineralization is associated with replacement, vein and matrix breccia styles of pyrrhotite mineralization which, through their distribution and structural zonation, appear to have developed synchronous to late with respect to Dn.

SULPHIDE DISTRIBUTION

Bounty Horizon

Pyrrhotite is the dominant sulphide mineral within the Bounty Horizon and its distribution suggests it was introduced during the Dn shearing event. Pyrrhotite abundances (visually estimated volume percent) vary from 1–2% for the weakly deformed zone, between 5 and 20% for the moderately deformed zone, and between 20 and 60% for the strongly deformed zone (Appendix II). In the latter it occurs as disseminated grains replacing magnetite–rich bands, vein fill or as matrix to breccias. Within the weakly deformed zone, pyrrhotite is disseminated in magnetite–rich beds and generally occurs where a weak foliation or open folding has developed. Partial replacement of magnetite by pyrrhotite occurs in the weakly deformed and moderately deformed zones, while almost total replacement predominates in the strongly deformed zone.

Fractures, grain boundaries, and cleavage surfaces in quartz, magnetite, hedenbergite, grunerite, actinolite, biotite, garnet and arsenopyrite are locally filled by pyrrhotite (Fig. 22, Fig. 26, Fig. 27 and Fig. 28). Asymmetric pressure shadows developed around sheared hedenbergite selvages and amphibole or garnet porphyroblasts are also filled with pyrrhotite (Fig. 16, Fig. 27 and Fig. 28). Pyrrhotite is present on Sn cleavage surfaces in Fn hinge zones, in gentle plunging boudin necks and in micro–faults subparallel or oblique to So and Sn (Fig. 18, Fig. 20, Fig. 21 and Fig. 22). Tension fractures and conjugate micro–faults oriented near normal to both the undeformed bedding or mylonitic Sn and Ln fabrics are filled with pyrrhotite (Fig. 24 and Fig. 29).

Pyrrhotite-rich veins with a massive pyrrhotite-matrix and floating clasts of deformed iron formation or co-precipitated calc-silicates, calcite or quartz form a breccia texture (Fig. 19; see following section on pyrrhotite-matrix breccias). Pyrrhotite-matrix breccias develop within zones of strong foliation and transposition, in Fn hinge zones, boudin necks, micro-faults and tension fractures as described above. The matrix pyrrhotite has a subgranoblastic texture and some deformation twins (Caswell, 1989).

Minor amounts of pyrite and marcasite, arsenopyrite, chalcopyrite and sphalerite occur with the vein, matrix breccia and replacement styles of pyrrhotite mineralization (Fig. 40). Pyrite and marcasite are abundant in the oxidized upper levels, but are minor at depth. Most pyrite and marcasite occurs as subhedral and euhedral grains with rare grains containing inclusions of pyrrhotite and gold. Pyrite and marcasite replaces pyrrhotite, often retaining its breccia texture. Pyrite in the chloritic contact shear contains fractures infilled with chlorite (Fig. 37). Arsenopyrite is subhedral to euhedral and contains fractures filled with pyrrhotite, sphalerite and chalcopyrite (Fig. 40).

Late-Dn quartz veins with visible gold contain disseminated pyrrhotite, pentlandite, molybdenite and chalcopyrite (Fig. 35). Vein selvages mainly consist of disseminated pyrrhotite.

The strong correlation of pyrrhotite distribution with Dn strain partitioning in the Bounty Horizon and its occurrence along Sn, in Fn hinge zones, in tensional structures normal to Ln and Sn, and in Dn pressure shadows around porphyroblasts indicate sulfide mineralization occurred during Dn. However, the occurrence of pyrrhotite in tensional fractures normal to Ln and crosscutting mylonitic Sn fabrics suggests shearing (Dn) without mineralization was active at some localities which, with time, became mineralized. As such, shearing is a progressive event and pyrrhotite mineralization is described as synchronous to late with respect to Dn.

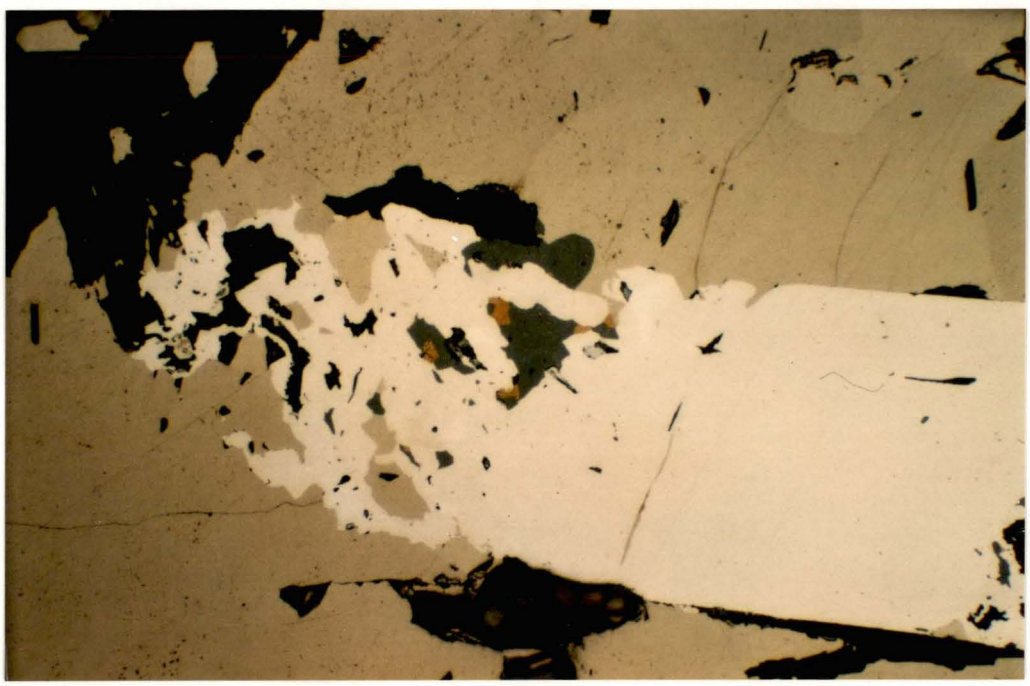

Figure 40. Photomicrograph of matrix pyrrhotite with sphalerite and chalcopyrite surrounding subhedral arsenopyrite grain. Pyrrhotite sphalerite and chalcopyrite also occur as veins and inclusions in arsenopyrite (318028, photo length = .3mm, reflected light)

Intrusion of the Proterozoic Binneringie Dyke across the mineralized Bounty Horizon oxidized most pyrrhotite to magnetite within 100 metres of its contact (Caswell, 1989).

Footwall Komatiitic Volcanics

As previously described, pyrite ± pyrrhotite(?) occurs in, and associated with, deformed quartz ± actinolite veins located within footwall komatiitic volcanic rocks adjacent to the Bounty Horizon. These veins have been folded during movement along the footwall shear zone. The timing of pyrrhotite, which occurs disseminated throughout the sheared komatiites, is not determined. Footwall rocks are, however, weakly mineralized in gold (Fig. 6), suggesting the pyrrhotite may have been introduced during sulfidation of the Bounty Horizon.

GOLD DISTRIBUTION

Economic gold mineralization is stratabound within the sheared Bounty Horizon. Gold mineralization occurs with late-Dn quartz veins and syn- to late-Dn vein, matrix breccia, and replacement styles of pyrrhotite mineralization. These have mineral clasts, vein minerals and/or selvages of hedenbergite, calcite, actinolite, Ca-plagioclase, quartz, clinozoisite, biotite, hornblende and apatite in varying proportions and assemblages. Gold grades also show a good correlation with strain zonation through the Bounty Horizon, thus timing the mineralization as a Dn event. Highest grades of mineralization occur in the strongly deformed, strongly sulphidic zone of the hanging wall shear while only minor gold mineralization (<0.5ppm) occurs in the weakly deformed, weakly sulphidic zone (Fig. 6). Gold grades through the moderately deformed zone are also greatest in the discrete zones of strong foliation and pyrrhotite mineralization. The chloritic contact shear zone is weakly mineralized in gold, although grades increase where clasts of iron formation or gold-bearing quartz veins are present.

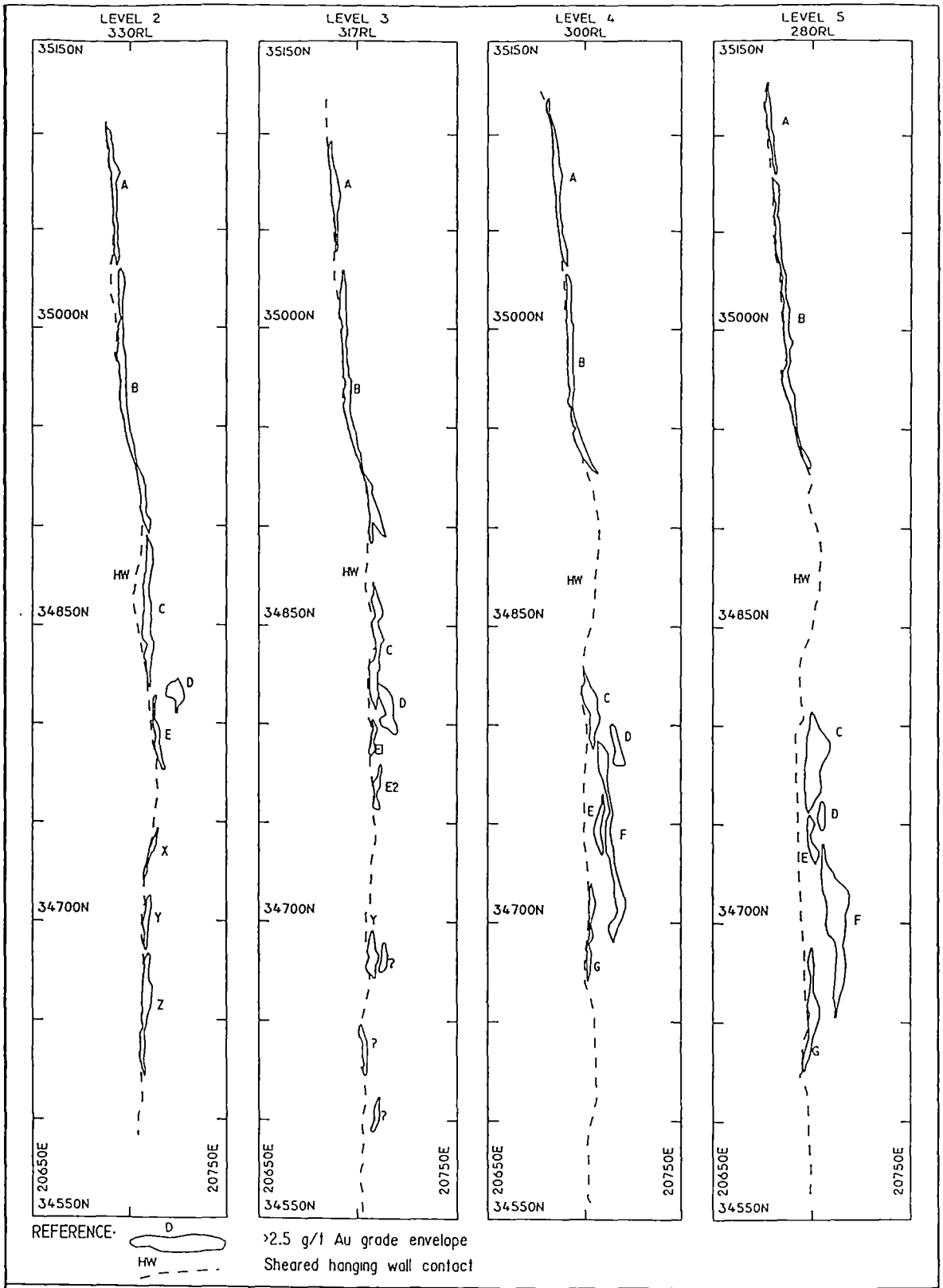

Scale:	1:2,500		Aztec Mining Company Limited
Author:	R A. RUTHERFORD	Date. 21 FEB 1992	
Drawn:	R.A. NICOL	Date. 21 FEB 1992	BOUNTY LEVEL PLANS SHOWING POSITION OF SHEARED HANGING WALL BOUNDARY AND >2.5 g/t GOLD GRADE ENVELOPE
Figure 41			

Economic gold mineralization mostly occurs within the hanging wall shear zone. However, below level 4 and south of 34850N a significant zone of mineralization is developed in sheared Bounty Horizon adjacent to the footwall contact (Fig. 41, grade envelopes D, E and F). The footwall lodes mainly consist of vein quartz with visible gold and associated haloes of hedenbergite and pyrrhotite. Mine observations and grade level plans suggest that mineralization is controlled by the favourable strike orientation of the sheared footwall contact (discussed further in the section on gold grade contours). A more detailed study of the footwall mineralization is required.

Pyrrhotite–Matrix Breccia

Deformation of the iron formation shows a direct correlation with pyrrhotite mineralization. The presence of pyrrhotite alone is, however, not an indication of economic gold grades as both gold–rich and gold–poor breccias with a pyrrhotite matrix are observed.

Gold–rich breccias contain mineral clasts of hedenbergite, calcite, plagioclase, quartz and actinolite or hornblende (blue–green coloured) with minor biotite and accessory apatite (Fig. 42 and Fig. 43). Some plagioclase clasts appear fractured and pyrrhotite develops a net texture where calcsilicates or calcite comprises about 50–70% of the assemblage (Fig. 43). Mineral clasts within the gold–poor breccias essentially consist of quartz and actinolite with some biotite and clinozoisite (Fig. 44). Deformed iron formation clasts appear to be more abundant in the gold–poor breccias and are partly altered to assemblages containing actinolite, biotite and clinozoisite (Fig. 19 and Fig. 45). Hedenbergite–rich vein assemblages with minor interstitial magnetite and pyrrhotite are also observed in areas of poor mineralization.

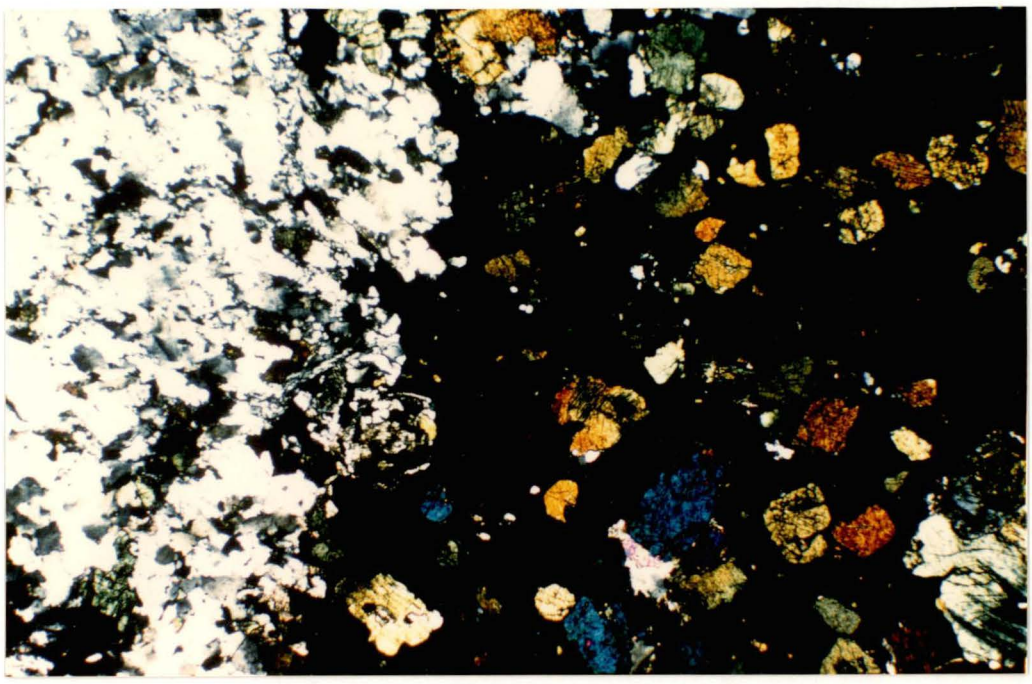

Figure 42. Photomicrograph of gold-rich pyrrhotite-matrix breccia. Pyrrhotite (black) with mineral clasts of hedenbergite, plagioclase, calcite and quartz. Note pyrrhotite-matrix breccia cuts across quartz with a partially recrystallized ribbon (mylonite) texture (318625, photo length = 6.7mm, xpl)

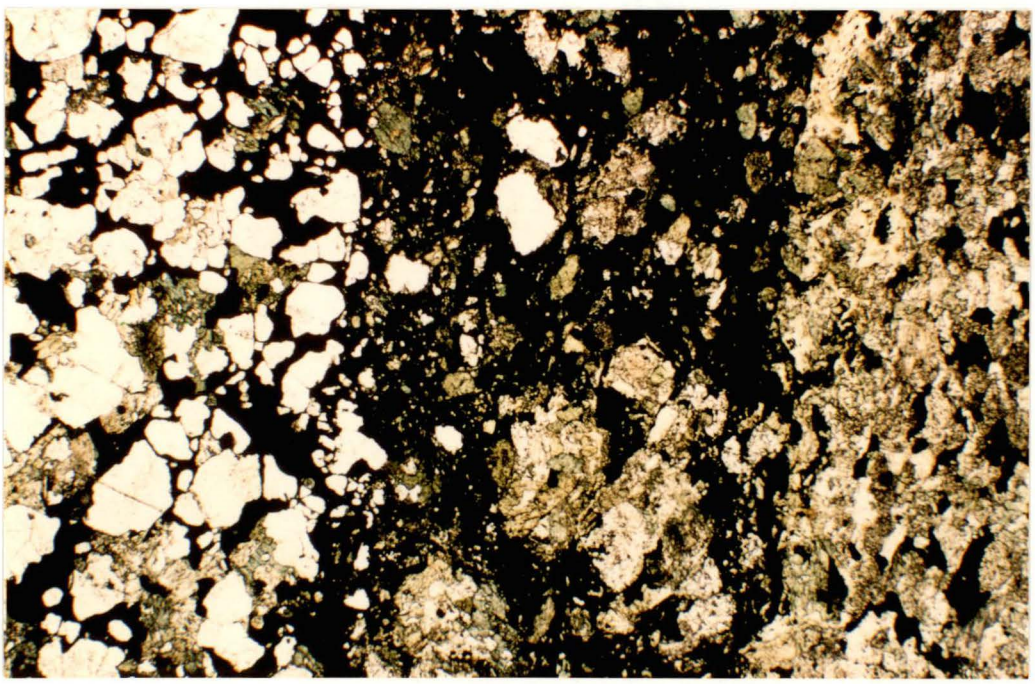

Figure 43. Photomicrograph of gold-rich pyrrhotite-matrix breccia showing some typical variations in the proportion of mineral clasts to pyrrhotite and mineral clast assemblages. Note the assemblage with abundant Ca-plagioclase, minor hedenbergite, calcite and actinolite, and net textured pyrrhotite (left); the assemblage with abundant calcite, actinolite and hedenbergite with minor pyrrhotite (right); and the pyrrhotite-rich assemblage with floating clasts of actinolite, calcite, hedenbergite and Ca-plagioclase (centre) (318631, photo length = 6.7mm, ppl)

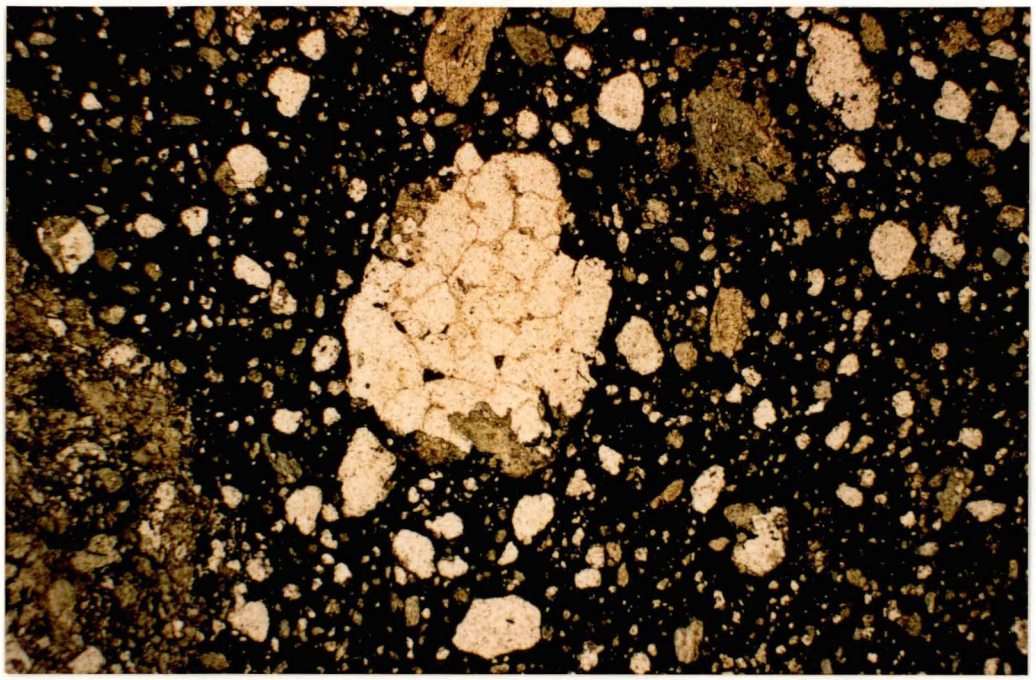

Figure 44. Photomicrograph of a gold-poor pyrrhotite-matrix breccia with floating mineral clasts of quartz and actinolite (318622, photo length = 3.5mm, ppl)

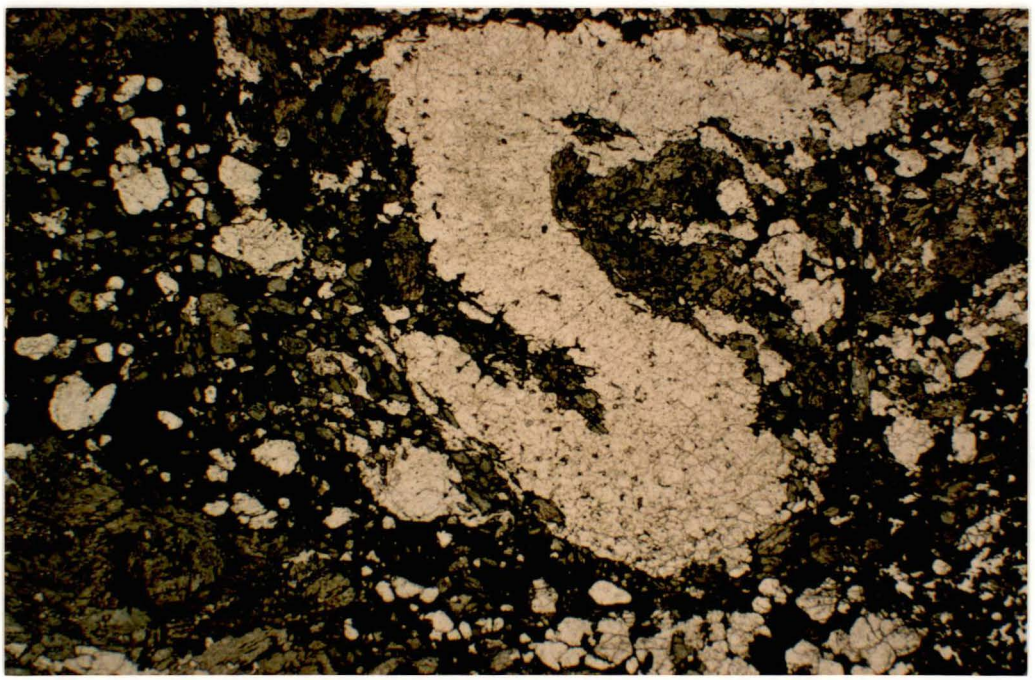

Figure 45. Photomicrograph of a gold-poor pyrrhotite-matrix breccia (black) with floating mineral clasts of quartz and actinolite. Note the net textured pyrrhotite and the Fn structure which was partially destroyed during the introduction of pyrrhotite (318629, photo length = 6.7mm, ppl)

Observations, though not thermodynamically constrained, suggest the solubility of hedenbergite, calcite and Ca-plagioclase affects the composition of the ore fluid and may be important parameters in controlling the solubility of gold.

Hanging Wall Shear Zone

The sheared hanging wall boundary of the Bounty Horizon is marked by the distinctive chloritic contact shear which has been mapped in detail by mine geologists I. Chen and D. Buchanan. Using this information, a long section showing form contours of the shear as projected onto a reference plane was constructed (Connelly Diagram). The reference plane strikes north-south, dips 75° west and has a grid reference on level 1 of 35120N 20674.5E. Distance between the reference plane and the shear was measured every 10 metres along drives 1 through to 5 inclusive (Appendix III). Position of the sheared hanging wall boundary is conjectual south of 34750N in drives 4 and 5 and from about 34780N to 34700N in drive 3. Long sections highlighting changes in strike and apparent dip angle of the hanging wall shear relative to the reference plane were also constructed. These sections are compared with a contoured long section of gold grade within sheared Bounty Horizon adjacent to the hanging wall boundary (Appendix III, Fig. 46).

Form Diagram (Connelly Diagram)

Highest contour values on the long section represent areas furthest from the reference plane. Data show a broad buckle in the shear centred about 34900N (Fig. 46). North of 34900N, the shear plane strikes west of north and steepens in a southwesterly dip direction. To the south, the shear becomes near parallel to the reference plane and steepens in an easterly dip direction.

Changes in Strike

The difference between adjacent form variables in the horizontal direction (S) were calculated along each drive.

$$S(L) = D(n-10) - D(n)$$

where D(n) is the distance along level L between reference plane and shear at northing n; D(n–10) is the distance along level L between reference plane and shear at northing n minus 10 metres; and S(L) is the difference along level L between adjacent variables D(n–10) and Dn.

This method of analysis effectively mapped changes in strike of the hanging wall shear relative to the reference plane such, that the larger S, the greater the strike deviation from north.

$S = 0$ strike of shear parallel to strike of reference plane (north).

$S > 0$ strike of shear west of north.

$S < 0$ strike of shear east of north.

Results highlight a sharp change in strike from S>1 to S<1 at about 34900N (Fig. 46). Between 34920N and 34940N, a large positive S up to 4.7 metres is observed. A large negative S down to 3 metres occurs between 34850N and 34860N.

Changes in Apparent Dip

The difference between adjacent form variables in the vertical direction (A) were calculated.

$$A(n) = D(L+1) - D(L)$$

where D(L) is the distance at northing n between reference plane and shear on level number L (numbers 1 through to 5); D(L+1) is the distance at northing n between reference plane and shear on level number L+1; and A(n) is the difference between D(L+1) and D(L) at northing n.

This method of analysis mapped changes in apparent dip angle of the hanging wall shear relative to the reference plane.

$A = 0$ apparent dip angle of shear at northing n is equal to the dip angle of the reference plane (75° west).

$A > 0$ apparent dip angle of shear at northing n is steeper than the dip angle of the reference plane.

$A < 0$ apparent dip angle of shear at northing n is shallower than the dip angle of the reference plane.

Contouring the A(n) data show a large surface area of the shear with an apparent dip angle, relative to the reference plane, of greater than 75° (Fig. 46). The shear has an apparent dip angle of less than 75° from about 34850N to 34700N. Contours, although limited by the vertical extent of data, reflect buckle folding of the shear surface with subhorizontal to gentle southwards plunging axes (Fig. 36).

Gold Grade Contours

A long section showing contoured gold grade data from 10 metre stope blocks over 6 levels has been compiled by mine geologist Duncan Buchanan. Contours illustrate the steep plunge and anastomosing distribution of the gold mineralization.

Visual comparison of gold grade with the form diagram (Fig. 46) suggests some correlation of grade with strike of the sheared hanging wall contact. An area of gold grades less than 2.5g/t occurs about the major bend in the shear located between 34850N and 34900N.

Visually, a strong correlation of contour shape and magnitude exists between the gold grade long section with that illustrating strike changes in the hanging wall shear; particularly north of 34750N (Fig. 46). South of 34750N, the shear position is conjectual and mineralization is complicated by a footwall lode. Gold mineralization

greater than 5g/t Au appears coincident with positive S values less than 3 or localized negative S values greater than -0.5. Negative S values less than -1.5 and S values greater than 3 appear coincident with areas of low grade (less than 2.5g/t Au). For S values between 0.5 and -1.5, grades less than about 5g/t Au are more common, however, local variations in grade from greater than 2.5g/t Au to less than 10g/t Au occur. This variance between the long sections may reflect differences in sample spacing or inaccuracies in positioning of the shear. Contour shapes and magnitudes showing good correlation are highlighted on the long sections (Fig. 46, Appendix III).

A. North plunging shoots of S >1 with >10g/t Au contours from 35110N to 35050N.

B. Low grade tongue of -0.8 >S <0 with <10g/t Au contour over levels 1 to 3 from 35000N to 35070N.

C. Broad, steep plunging zone of S >0.5 with >10g/t Au contour from 34900N to 35020N.

D. Thin, steep plunging zone of S >3 with <2.5g/t Au contour over levels 4 and 5 from 34920N to 34930N.

E. Steep plunging 0.5 and 0 S contours with 15g/t Au and 10g/t Au contour over levels 2, 3 and 4 between 34950N and 34975N.

F. Broad zone of S <0 and S <1.5 with <5g/t Au and <2.5g/t Au contour from 34900N to 34830N over levels 3, 4 and 5.

G. Negative S value on level 5 (34990N to 35000N) appears coincident with a NW striking fault with a small dextral offset.

Strike control on the distribution of gold grade is also evident from the continuity of the greater than 2.5g/t gold grade envelopes viewed on level plans (Fig. 41). Where the sheared hanging wall boundary strikes between 4° and 8° west of north, grade envelopes are continuous over 50 to 200 metres and occur adjacent to the sheared boundary. Thin grade envelopes continuous over about 20 to 50 metres are developed along the sheared hanging wall boundary where it strikes between 0° and 5° east of north and greater than 8° west of north. The footwall envelopes which also strike between about 4° and 8° west of north (Fig. 41), appear to have developed where the sheared footwall boundary was in this favourable strike orientation. Gold grade on the bend in the shear hanging wall boundary situated between 34850N and 34930N is generally less than 2.5g/t (Fig. 41 and Fig. 46 location F).

Changes in the apparent dip angle between the reference plane and the sheared hanging wall contact show a poor correlation with gold grade (Fig. 46). Data show buckle folding of the shear surface with subhorizontal to gentle south plunging axes. Buckling is interpreted to have developed during Dn which is characterized by the development of asymmetric folds plunging gently towards the south (Fig. 36).

METAMORPHISM AND ITS RELATIONSHIP TO DEFORMATION

Mineral assemblages and their overprinting relationship with respect to Dn fabrics indicate that metamorphism of lower amphibolite facies was active before and continued after shearing ceased.

Peak metamorphic assemblages in unmineralized Bounty Horizon mainly comprise grunerite – magnetite – quartz in variable proportions, magnetite – biotite, magnetite plagioclase (rare) and biotite – garnet (almandine) ± hornblende ± quartz (Fig. 8). These minerals are pre–Dn and define a bedding parallel foliation (Sn), occur in folded beds and, less commonly, define a folded foliation (Fig. 21). All locally contain pyrrhotite in some cleavages or fractures.

Figure 46. Contoured long sections highlighting the form and changes in the orientation of the sheared hanging wall boundary of the Bounty Horizon (over mining levels 1 through to 5 inclusive); and the gold grade distribution within sheared Bounty Horizon adjacent to the hanging wall boundary (see text and Appendix III for details)

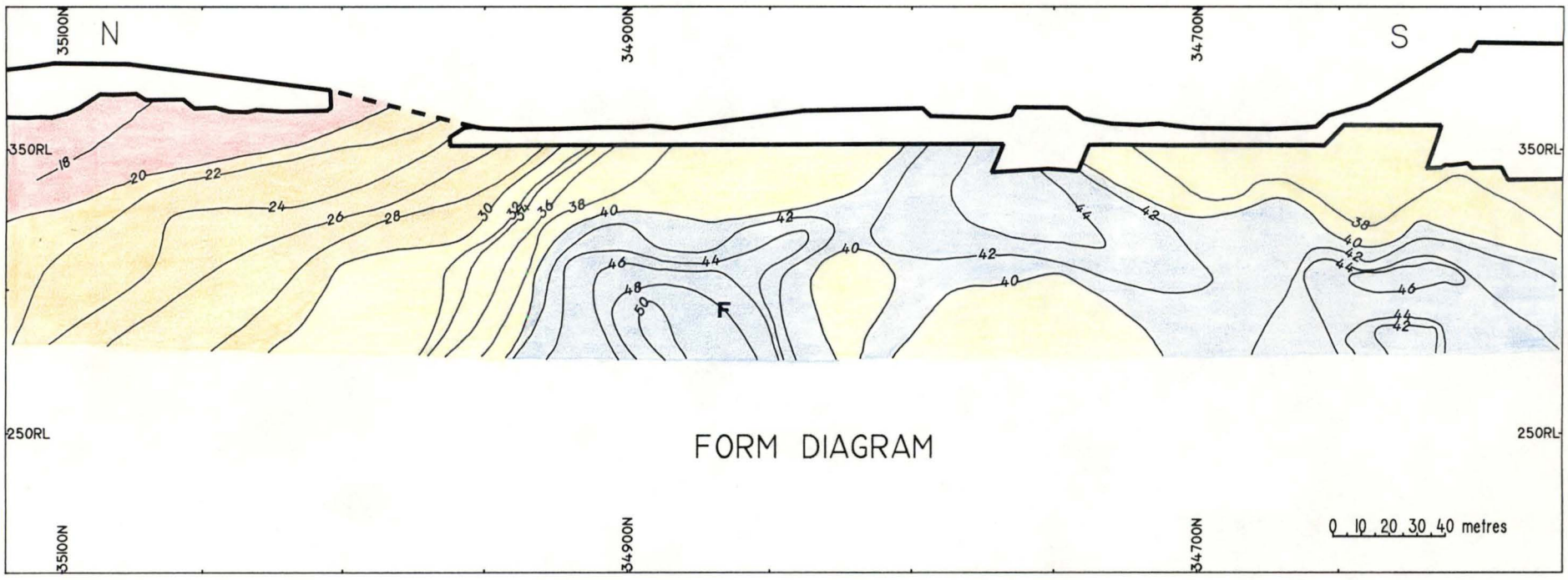

FORM DIAGRAM

D(m)

50

40

30

20

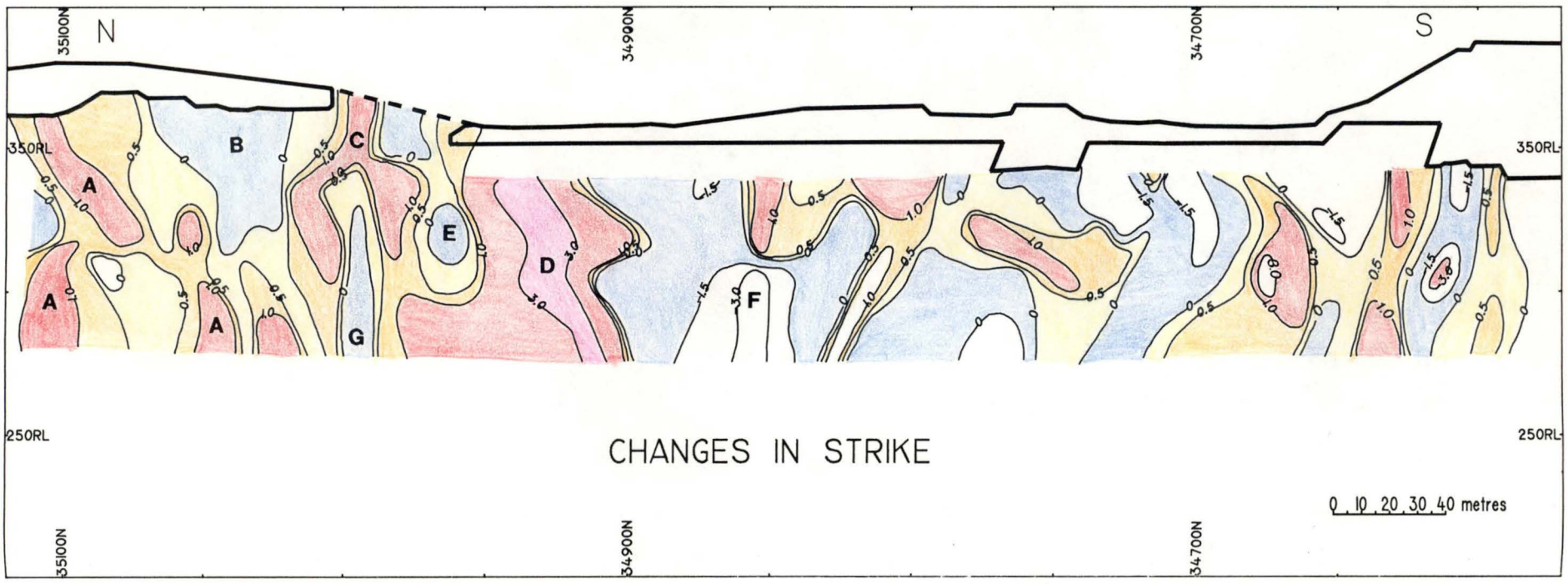

CHANGES IN STRIKE

Δ S(m)

3.0

1.5

1.0

0.5

0

-1.5

-3

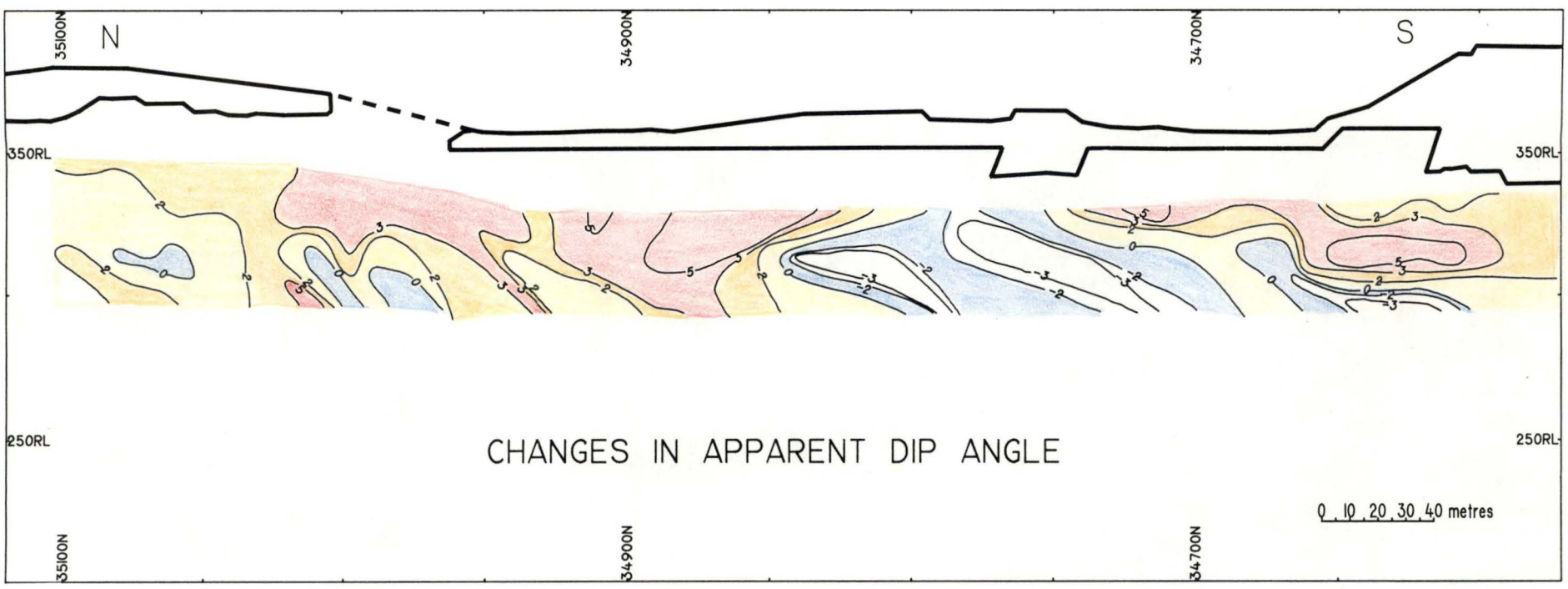

CHANGES IN APPARENT DIP ANGLE

Δ A(m)

5

3

2

0

-2

-3

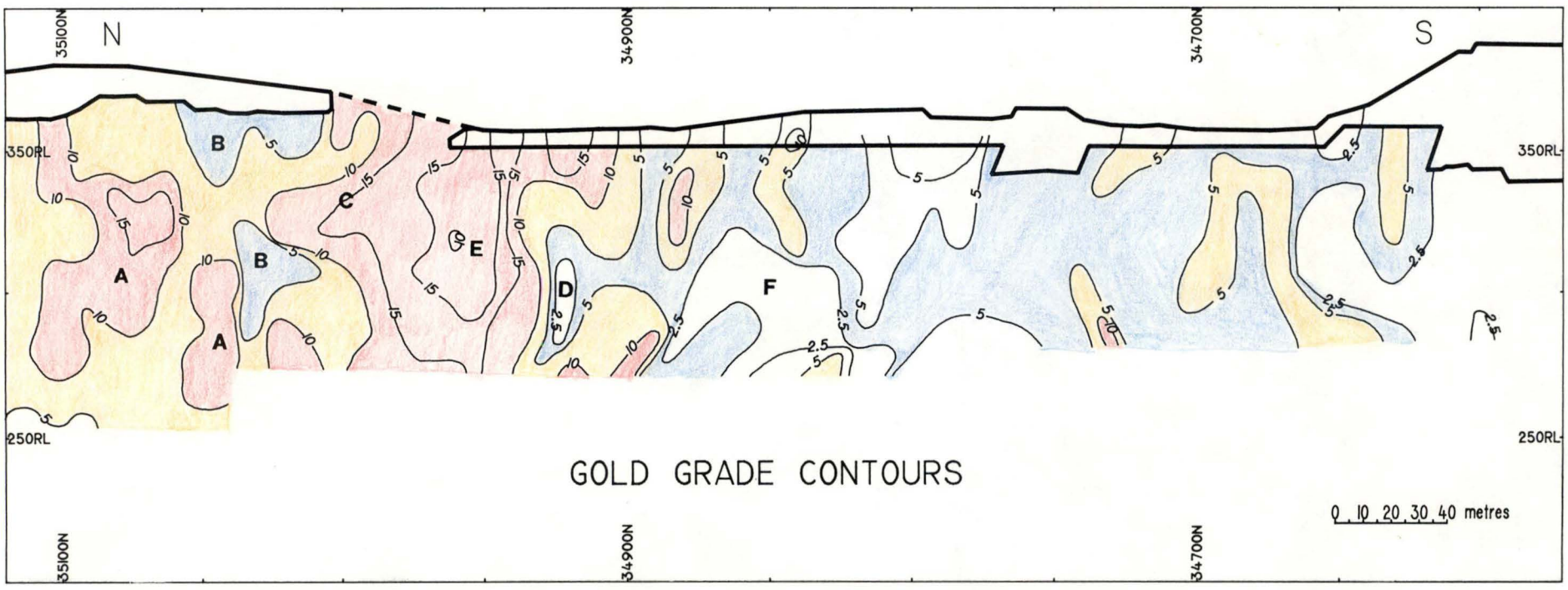

GOLD GRADE CONTOURS

Au(ppm)

15

10

5

2.5

0

Garnets occur as euhedral undeformed porphyroblasts overgrowing foliated biotite–rich beds (Fig. 22) or as folded and rotated porphyroblasts in crenulated biotite–rich beds (Fig. 27, Fig. 28 and Fig. 47). Deformed garnet, hornblende and ferro–actinolite porphyroblasts occur along Sn axial planar to Fn structures (Fig. 48 and Fig. 50). Garnet porphyroblast growth appears therefore to be post D_{n-1}, pre–Dn and syn–Dn. These characteristics may be typical of syntectonic porphyroblast growth controlled by shifting patterns of strain partitioning during progressive shearing (Bell and Fleming, 1985). All of the garnets described above have fractures infilled with pyrrhotite (Fig. 49).

Amphibole growth and peak metamorphism appears to have continued after Dn and pyrrhotite – gold mineralization. Randomly oriented actinolite porphyroblasts within footwall komatiites, grunerite and actinolites in the Bounty Horizon overprint Sn and Ln (Fig. 13). Late–Dn peak metamorphic conditions also resulted in the local development of granoblastic quartz and subgranoblastic pyrrhotite textures within the strongly deformed zone. Recrystallization of fine–grained So in the weakly deformed zone developed a radiating grunerite texture around coarse–grained subhedral magnetite cored with pyrrhotite.

Hedenbergite is considered to be a vein mineral and not part of the original peak metamorphic assemblage. It occurs as deformed selvage and vein mineral in early–Dn quartz – calcite – hedenbergite ± garnet ± apatite veins (Fig. 16), as undeformed selvages or mineral clasts in pyrrhotite–matrix breccias and pyrrhotite veins (Fig. 42 and Fig. 43), or as selvages and vein minerals around the late–Dn quartz veins with visible gold (Fig. 34). Extreme deformation of early–Dn veins has developed a quartz mylonite with augens of magnetite and hedenbergite defining Sn and Ln (Fig. 25). During Dn, asymmetric pressure shadows filled with pyrrhotite around the early–Dn hedenbergite selvages (Fig. 16). Most early–Dn hedenbergite augens have been affected by peak metamorphic conditions and are partially replaced by grunerite (Fig. 17).

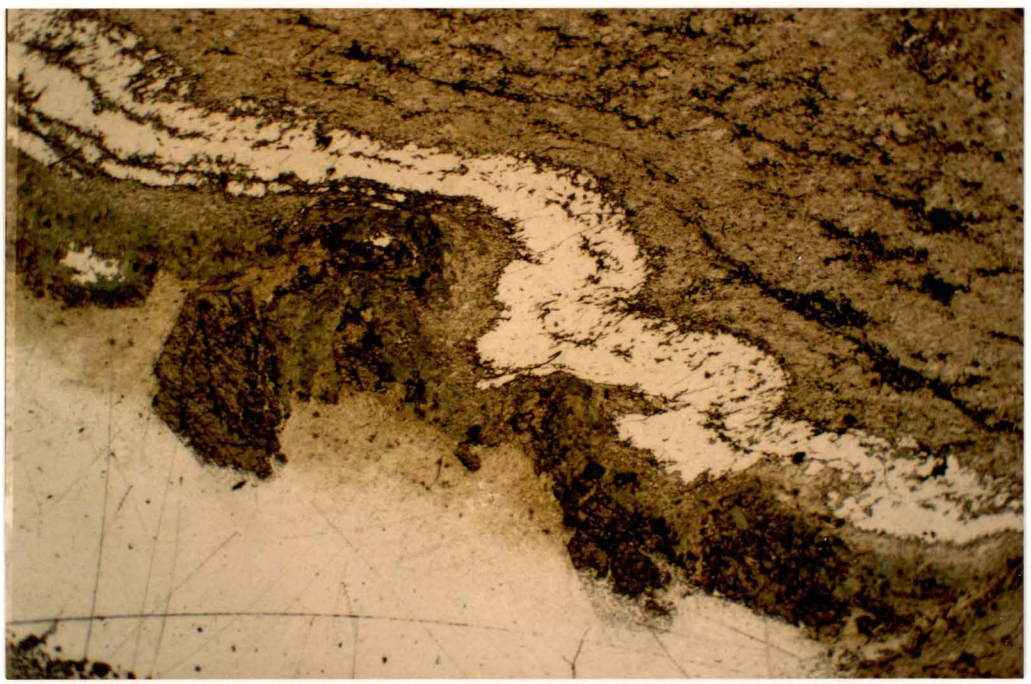

Figure 47. Photomicrograph of asymmetric Fn structures viewed facing south. Asymmetry consistent with formation of the fold during west-down normal shear movement along shear surfaces parallel to So (steep west). Note the crushed and folded garnets (pre-Dn) within the lower biotite-rich bed (518022, photo length = 6.7mm, ppl)

Figure 48. Photomicrograph of Fn structure with an axial planar Sn fabric developed in quartz-rich bed. Garnet and hornblende developed along Sn (central black zone) (318021, photo length = 13.5mm, ppl)

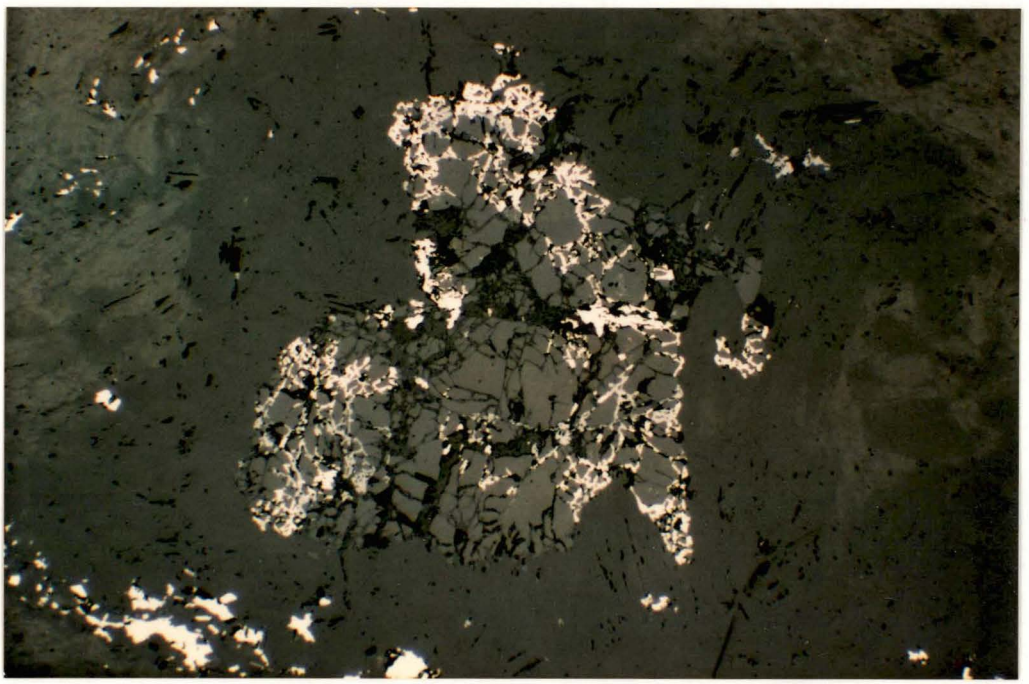

Figure 49. Photomicrograph of fractured garnet along Sn (from Fig. 48). Fractures infilled with pyrrhotite and sphalerite (318021, photo length = 1.3mm, reflected light)

Figure 50. Photomicrograph of Fn structure with an axial planar Sn fabric developed in quartz-rich and amphibole-rich beds. Actinolite (dark green) replacing grunerite (light green) along Sn (318020, photo length = 13.5mm, ppl)

Grunerite is replaced by ferro-actinolite during a period Ca-metasomatism (Caswell, 1989). Replacement occurs along Sn timing the metasomatism with the shearing and the gold mineralizing events (Fig. 50). Pyrrhotite along fractures or cleavages within some ferro-actinolite suggests it may pre-date the pyrrhotite-gold mineralizing event.

Metamorphism succeeding Dn includes chloritisation associated with D_{n+1} and oxidation of Bounty Horizon pyrrhotite to magnetite adjacent to the Proterozoic Binneringie Dyke.

SUMMARY

Deformation in pre-Dn times was dominated by strong east-west directed compression, which resulted in complex upright folding and thrusting of the supracrustal sequence (D_{n-1}). With cessation or relaxation of the compression, batholiths, plutons and porphyritic stocks, sill and dykes of granite-granodiorite composition were emplaced (Fig. 51). These have characteristic magnetic signatures and shapes and occur within and along the margins of the greenstone belt, and along some of the regional-scale thrusts. The intrusive suite is interpreted as pre-Dn.

A pre-Dn pluton was intruded adjacent to the eastern side of the belt, about 800 metres northeast of the Bounty Deposit. The intrusion truncated and rotated greenstone stratigraphy adjacent to its margin (Fig. 3 and Fig. 4). In the Bounty Mine area, the host rocks were intruded by porphyritic dykes and locally rotated west of north (Fig. 52) during and as a result of the pluton's emplacement.

The bulk movement history of the Bounty Shear indicates that a vertically oriented maximum compressive stress (Dn) succeeded the pre-Dn intrusive event. Gravity-driven sagging of the greenstone pile or east-west directed extension following the regional east-west compression are possible causes of the vertically

oriented stress. As a result, strain was focused along existing deformation zones, rheologically contrasting rock boundaries and margins of pre-Dn intrusives. Shear zones with a normal movement sense developed along the footwall and hanging wall boundaries of the Bounty Horizon and early-Dn veins were intruded.

As normal shear movement progressed, these early veins, together with the peak metamorphic mineral assemblages, were aligned defining Sn parallel to bedding and Ln oriented down dip (Fig. 52).

Detailed form and orientation analysis of the sheared hanging wall boundary has shown areas of high grade gold mineralization to be controlled by its strike orientation. High grade, permeable zones of the shear appear to strike between about 4° and 8° west of north. Low grade, less permeable zones of the shear appear to strike between 0° and 5° east of north and greater than about 8° west of north.

The hanging wall boundary of the Bounty Horizon, locally rotated west of north during intrusion of a pre-Dn pluton, underwent down dip or steep oblique shear movement with a normal sense. The steep oblique movement translates in plan view to a lateral movement component, which had a sinistral sense. Sheared lithological boundaries striking between about 4° and 8° west of north were dilated, developing ore fluid pathways with a steep plunge. Results suggest the ore fluid pathways are, in part, controlled by the original shape of the Bounty Horizon's hanging wall boundary which was influenced by intrusion of the pre-Dn pluton located about 800 metres towards the northeast.

Dilation synchronous to late with respect to Dn deposited vein, matrix breccia and replacement styles of pyrrhotite-gold mineralization within the sheared Bounty Horizon. Dilation late with respect to Dn deposited quartz ± visible gold veins. For both types of mineralization, varying proportions and assemblages of actinolite, hedenbergite, Ca-plagioclase, hornblende, biotite, clinozoisite, calcite, quartz or apatite were deposited as vein minerals, mineral clasts and/or selvage. Grunerite was replaced by ferroactinolite during a period of Ca-metasomatism synchronous with Dn.

Differing chemical–physical conditions during dilation and mineralization have developed both gold–poor and gold–rich pyrrhotite–matrix breccias and quartz veins ± visible gold. Gold–rich pyrrhotite breccias and quartz veins with visible gold generally have mineral clast, vein mineral or selvage assemblages of hedenbergite, calcite, Ca–plagioclase, quartz, actinolite or hornblende in varying proportions with minor biotite and accessory apatite. Gold–poor pyrrhotite breccias and quartz veins with no visible gold have mineral clast, vein mineral or selvage assemblages of actinolite, quartz, biotite and clinozoisite in varying proportions with accessory apatite.

Following the termination of Dn and the gold mineralizing event, compositionally variable calc–silicate – calcite veins intruded the Bounty Mine sequence overprinting Dn structures and fabrics. Also, peak metamorphic conditions which coincided with Dn and the gold mineralizing event continued (Fig. 5). Evidence for syn–Dn and post–Dn peak metamorphic conditions include:

- the development of ferroactinolite, hornblende and garnet along Sn in Fn fold hinges;
- amphibole porphyroblasts overprinting Sn and Ln within footwall komatiites and Bounty Horizon;
- high temperature calc–silicate assemblages associated with syn–Dn to late–Dn gold mineralization; and
- post–Dn high temperature calc–silicate vein assemblages.

A weak regional deformation event (D_{n+1}) occurred after Dn (Fig. 5). The event is expressed as regional northwest trending fracture zones and faults or north–northwest trending zones of retrograde fracture cleavage intruded by quartz – epidote – chlorite ± calcite veins within the hanging wall gabbro. Steep plunging buckle folds within the Bounty Horizon and chloritization of the sheared hanging wall boundary are interpreted to have developed during this event.

Graphic textured granites and pegmatites intruded as flat dipping sheets or vertical dykes along D_{n-1}, Dn, D_{n+1} structures and other crustal weaknesses. The pegmatites and earlier formed structures and stratigraphy were cut across by east-northeast trending fracture zones which were intruded by Proterozoic dykes. Intrusion of the Proterozoic Binneringie Dyke across the mineralized Bounty Horizon oxidized most pyrrhotite to magnetite within 100 metres of its contact.

Figure 51. Summary of the tectono-thermal history and the timing of veins and gold mineralization within the geological setting of the Bounty Gold Mine

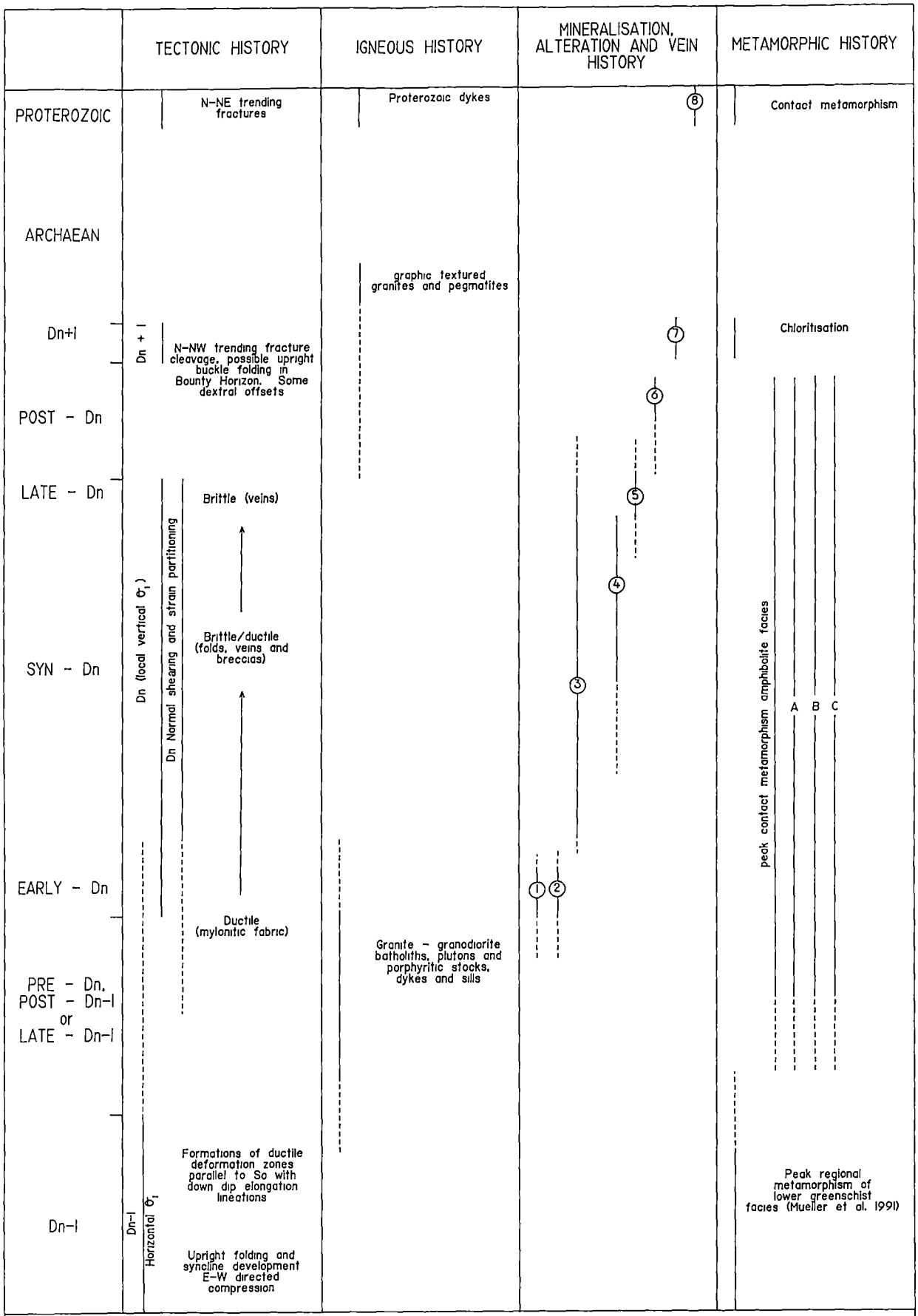

1. Pre to early-Dn quartz-pyrite+/-actinolite veins.
2. Pre to early-Dn quartz-calcite-hedenbergite+/-garnet+/-apatite+/-pyrrhotite? veins
3. Alteration of grunerite to ferro-actinolite, hornblende to biotite in gabbro.
4. Syn - Dn to late - Dn pyrrhotite veins and matrix breccias+/-gold with calcsilicate+/-calcite +/-quartz vein minerals and wall rock alteration Replacement of magnetite by pyrrhotite.
5. Late - Dn quartz-calcsilicate+/-calcite veins with pyrrhotite+/-visible gold+/-molybedenite+/-pentlandite +/-chalcopyrite and calcsilicate alteration assemblages
6. Post - Dn calcsilicate-calcite vein assemblages
7. Quartz-epidote +/- calcite veins with chloritic alteration haloes, chloritisation of sheared hanging wall contact, replacementof pyrrhotite by pyrite
8. Desulfidation of pyrrhotite forming magnetite adjacent Proterozoic dyke.

A Almandine growth

B Grunerite recrystallisation and replacement of hedenbergite

C Actinolite recrystallisation

Schematic illustration summarising structural elements controlling gold mineralisation within the Bounty gold deposit.

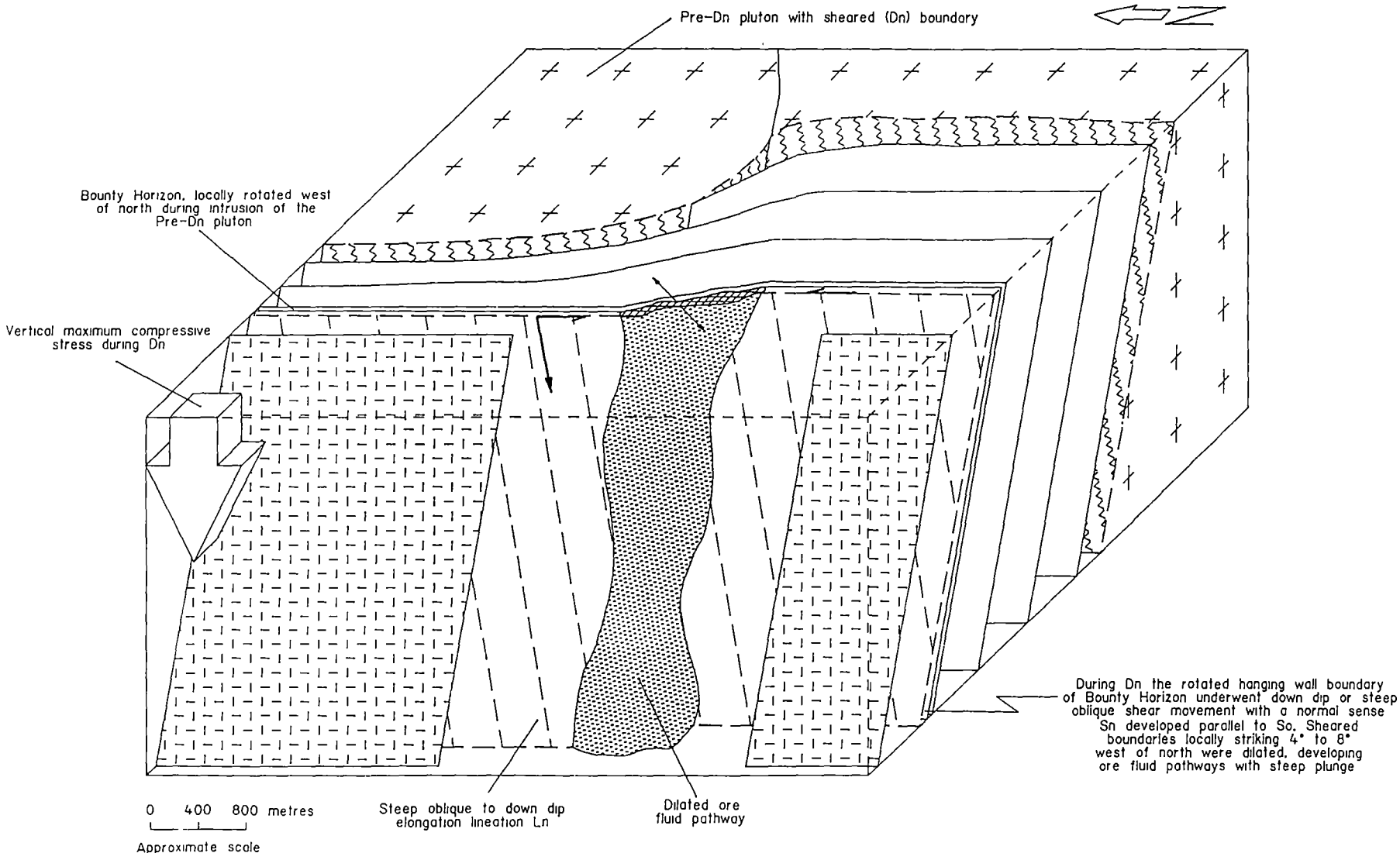

Figure 52

CONCLUSIONS

1. The Bounty orebody is bound within strata parallel shear zones which developed in an iron formation referred to as the Bounty Horizon during deformation event Dn. A footwall ultramafic volcanic sequence and a hanging wall gabbro bound the mineralized horizon which dips west between 70° and 90°.

2. Deformation in pre-Dn times was dominated by strong east-west directed compression which resulted in complex, upright folding and thrusting of the supracrustal sequence.

3. With cessation or relaxation of the east-west compression batholiths, plutons and porphyritic stocks, dykes and sills of granite to granodiorite composition were intruded into the folded greenstone sequence and broad contact metamorphic aureoles developed.

4. A period of vertically oriented, maximum compressive stress (Dn) succeeded the intrusive event. Resulting strain was focused along the footwall and hanging wall boundaries of the Bounty Horizon and shear zones with a normal movement sense developed.

5. The hanging wall boundary of the Bounty Horizon, which was locally rotated west of north during intrusion of a pre-Dn pluton, underwent down dip or steep oblique shear movement with a normal sense. The steep oblique movement translates in plan view to a lateral movement component, which had a sinistral sense. Sheared lithological boundaries striking about 4° to 8° west of north were dilated, developing ore fluid pathways with a steep plunge.

6. The ore fluid pathways are controlled by the rheological contrast and original shape of the Bounty Horizon's hanging wall boundary during Dn. The original shape was influenced by intrusion of a pre-Dn pluton located about 800 metres towards the northeast.

7. Differing chemical–physical condition during dilation and mineralization developed gold–rich and gold–poor pyrrhotite–matrix breccias and quartz veins ± visible gold.

8. Dn and the gold mineralizing event occurred during a peak contact metamorphic grade of lower amphibolite facies.

ACKNOWLEDGEMENTS

In completing this manuscript I would like to acknowledge and thank Dr Brett Davies for his unofficial supervisory role, comments and editing; Aztec Mining Company Ltd (Dr Bryan Smith) for financial and logistical support; and mine geologists Duncan Buchanan and Ivy Chen for access to the mine, grade plans and geological plans. Special thanks to Robert Nicol and Amanda Clarke for drafting of the diagrams and Sandy King for typing and editing of the text. Thank you also to Dr John Ridley and Dr Charter Mathison of the University of Western Australia for petrological assistance.

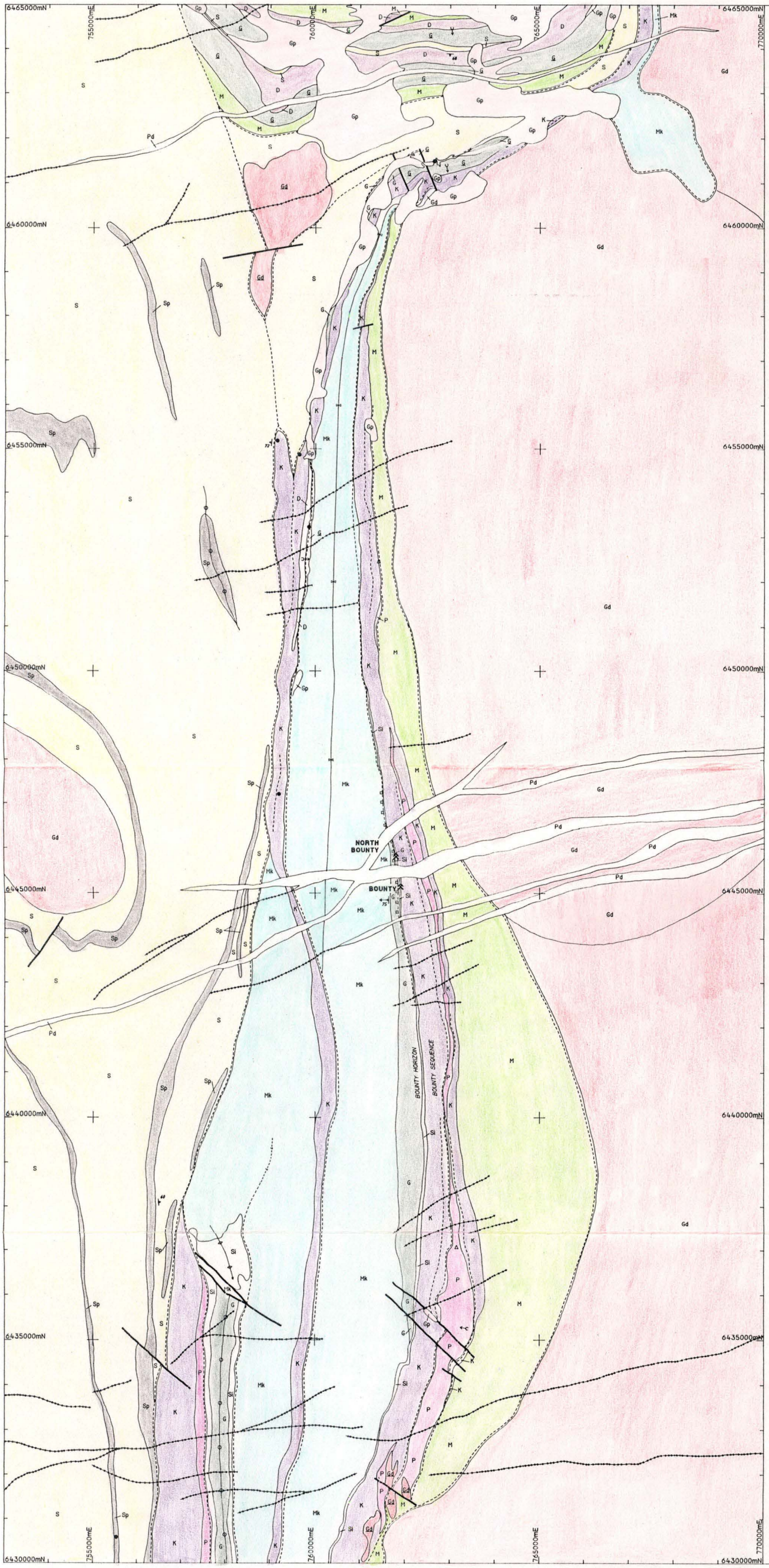

LITHOLOGICAL LEGEND

- Pd — Proterozoic dyke

ARCHAEAN

- Gp — Granite or pegmatite graphic textured microcline-quartz+/-muscovite+/-biotite, massive, low magnetic susceptibility
- Gd — Granite – granodiorite, deformed margins, high magnetic susceptibility. (porphyritic Gd)
- S — Pelitic and psammopelitic sediments
- Sp — Fe-rich, garnetiferous metapelites, with thin BIF and graphitic metapelites
- Si — Banded iron formation, magnetite, magnetite-silicate, chert and or garnetiferous metapelite beds
- M — Tholeiitic basalt and dolerite, high-magnesium basalt
- Mk — High-magnesium basalts and komatiitic basalts
- G — Gabbro, (pyroxenitic base G)
- D — Komatiitic peridotite or dunite overlain by pyroxenite and gabbro
- K — High-Magnesium basalts, komatiitic basalts, komatiitic peridotites+/-intercalations of chert, iron formation, Fe-rich pelite or psammitic sediments
- P — Komatiitic peridotite and dunite

LINEWORK SYMBOLS

- Interpreted geological boundary (based on outcrop, numerous drill spoils and aeromagnetic data)
- Interpreted ductile deformation zones (based on outcrop, numerous drill spoils and aeromagnetic data)
- Ductile deformation zone with normal movement sense (teeth on downthrown side)
- Fault
- Approximate strike and dip of bedding and parallel foliation
- Approximate strike and dip of bedding and parallel foliation with steep oblique to down dip elongation lineations and mineral lineations
- Direction of younging based on apparent differentiation trend in ultramatic sequence or individual flows
- Fold axis – unspecified
- Syncline axis
- Antiform axis
- Gold deposit
- Gold prospect
- Nickel prospect

GN

Scale 1:100 000

0 1 2 3 4 km

AUSTRALIAN MAP GRID ZONE 50

REGIONAL GEOLOGICAL SETTING OF THE BOUNTY GOLD MINE

Compiled by : R.A. Rutherford
Date : August 1992

Figure 3

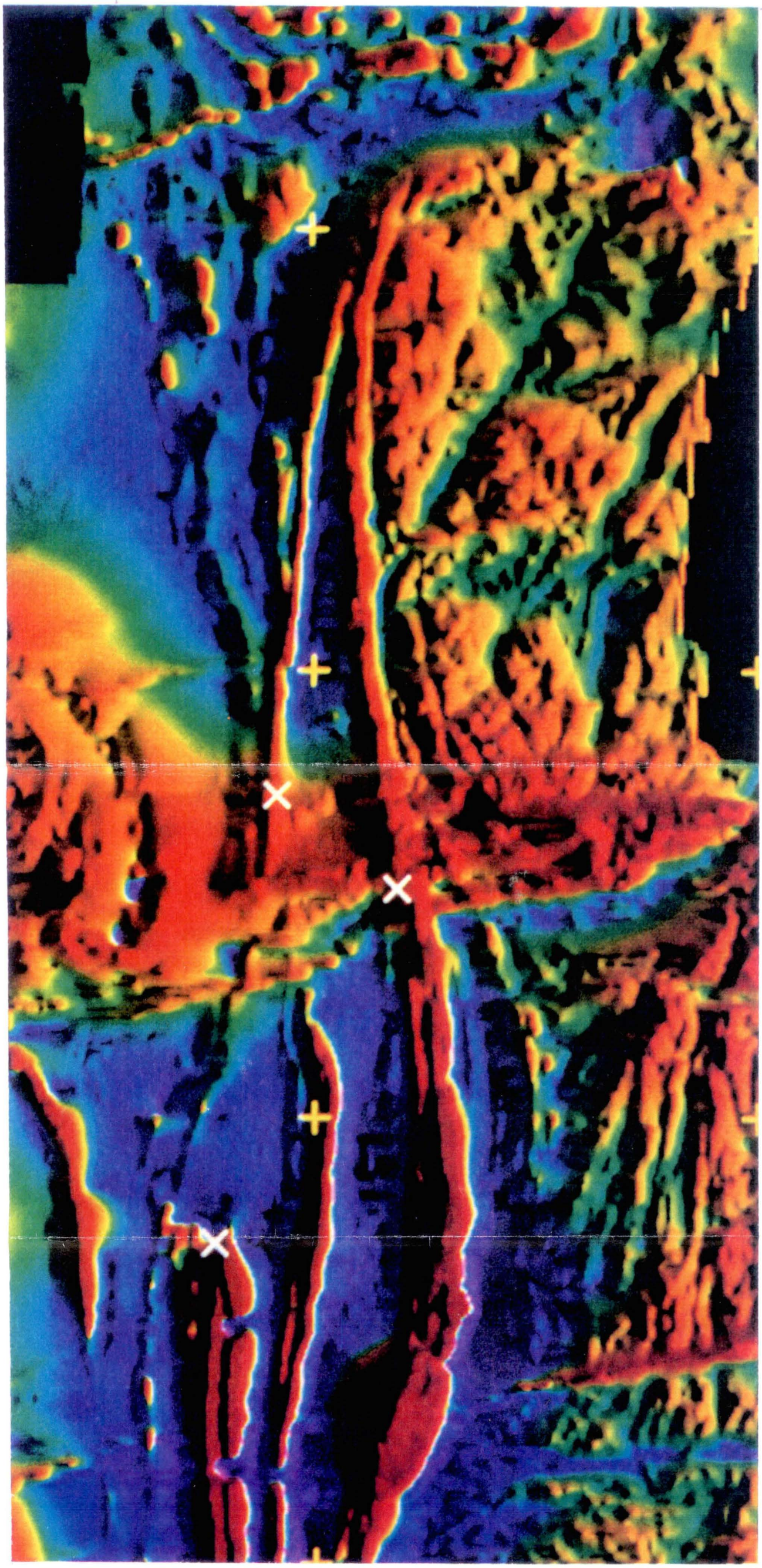

IMAGE PROCESSED AEROMAGNETIC DATA COVERING THE BOUNTY GOLD MINE

Figure 4

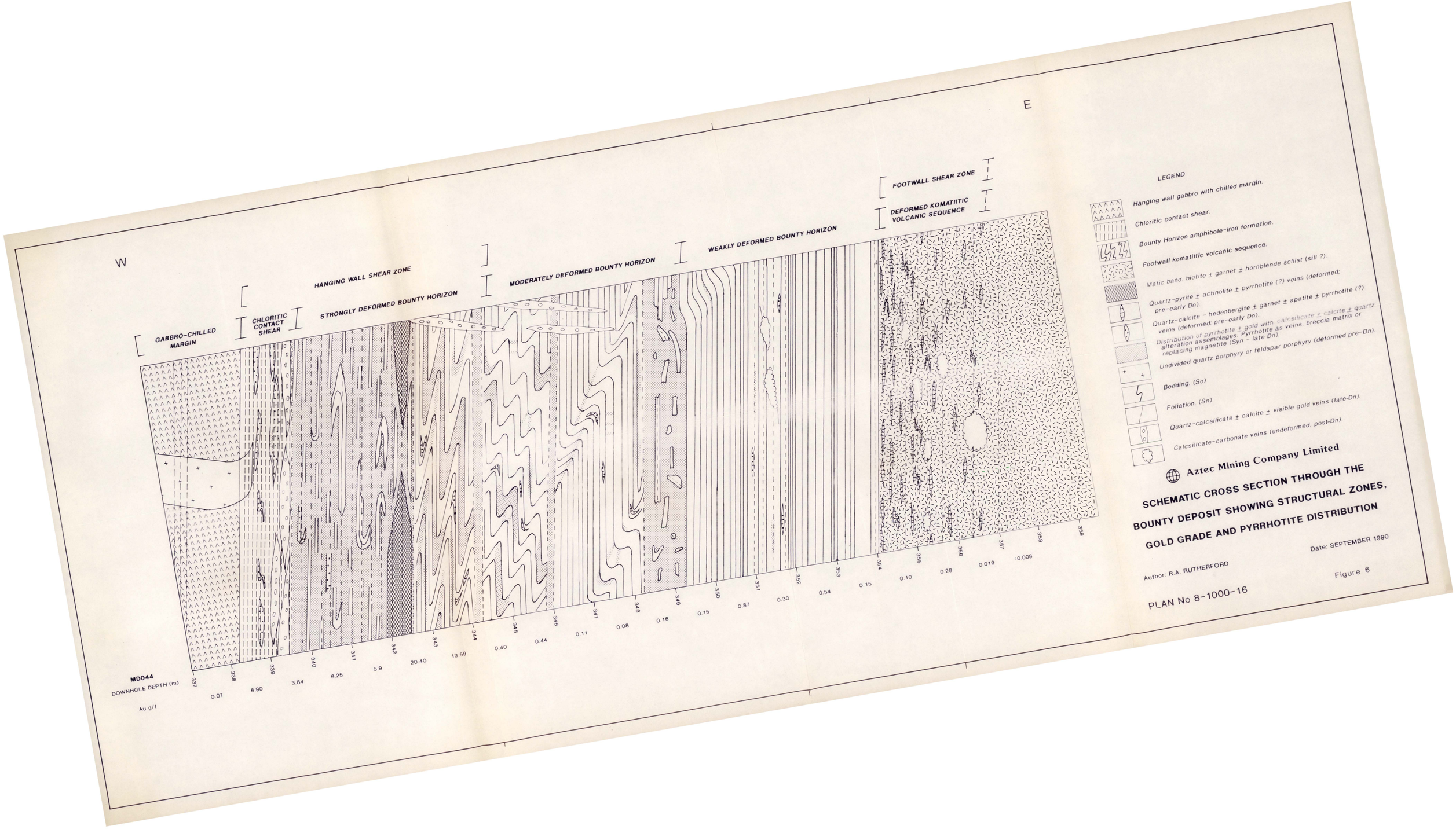
W
E
GABBRO–CHILLED MARGIN
CHLORITIC CONTACT SHEAR
HANGING WALL SHEAR ZONE
STRONGLY DEFORMED BOUNTY HORIZON
MODERATELY DEFORMED BOUNTY HORIZON
WEAKLY DEFORMED BOUNTY HORIZON
FOOTWALL SHEAR ZONE
DEFORMED KOMATIITIC VOLCANIC SEQUENCE
MD044
DOWNHOLE DEPTH (m)
337 338 339 340 341 342 343 344 345 346 347 348 349 350 351 352 353 354 355 356 357 358 359
Au g/t
0.07 6.90 3.84 6.25 5.9 20.40 13.59 0.40 0.44 0.11 0.08 0.16 0.15 0.87 0.30 0.54 0.15 0.10 0.28 0.019 <0.008
LEGEND
Hanging wall gabbro with chilled margin.
Chloritic contact shear.
Bounty Horizon amphibole–iron formation.
Footwall komatiitic volcanic sequence.
Mafic band: biotite ± garnet ± hornblende schist (sill ?).
Quartz–pyrite ± actinolite ± pyrrhotite (?) veins (deformed; pre–early Dn).
Quartz–calcite – hedenbergite ± garnet ± apatite ± pyrrhotite (?) veins (deformed; pre–early Dn).
Distribution of pyrrhotite ± gold with calcsilicate ± calcite ± quartz alteration assemblages. Pyrrhotite as veins, breccia matrix or replacing magnetite (Syn – late Dn).
Undivided quartz porphyry or feldspar porphyry (deformed pre–Dn).
Bedding. (So)
Foliation. (Sn)
Quartz–calcsilicate ± calcite ± visible gold veins (late–Dn).
Calcsilicate–carbonate veins (undeformed, post–Dn).
Aztec Mining Company Limited
SCHEMATIC CROSS SECTION THROUGH THE BOUNTY DEPOSIT SHOWING STRUCTURAL ZONES, GOLD GRADE AND PYRRHOTITE DISTRIBUTION
Date: SEPTEMBER 1990
Author: R.A. RUTHERFORD
Figure 6
PLAN No 8-1000-16

REFERENCES

Ahmat, A.L., 1986, Metamorphic patterns in the greenstone belts of the Southern Cross Province, Western Australia. Geological Survey of Western Australia, Professional Paper 19, p1-21.

Bell, T.H. and Fleming, P.D., 1985, Foliation development, porphyroblast nucleation and growth and deformation history, Jour. Struct. Geol., v. 7, p489-490.

Blight, D.F. and Barley, M.E., 1981, Estimated pressure and temperature conditions from some Western Australian Precambrian metamorphic terrains. Geological Survey of Western Australia, Annual Report for 1980, p67-72.

Caswell, M.J., 1989, Nature and timing of mineralisation at the Bounty Gold Mine: A BIF-hosted gold deposit in an amphibolite facies terrain. Honours thesis, Univ. West. Aust., 43p (unpubl).

Chin, R.J., Hickman, A.H. and Thom, R., 1984, Explanatory notes on the Hyden 1:250,000 geological sheet (SI 50-4), Western Australia. Geological Survey of Western Australia, Perth.

Davies, B., 1990, Structural history of the Forrestania Greenstone Belt, internal report No. 410, Aztec Mining Co Ltd, 11p (unpubl).

Gee, R.D., 1982, Explanatory notes on the Southern Cross 1:250,000 geological sheet (SH 50-16), Western Australia. Geological Survey of Western Australia, Perth.

Gole, M.J. and Klein, C., 1981, High-grade metamorphic Archaean banded iron-formation, Western Australia: assemblages with coexisting pyroxenes ± fayalite. American Mineralogist, v. 66: p87-99.

Martyn, J., 1988, Notes to accompany 1:25,000 preliminary geological interpretation maps, Sheets 1 to 3, Forrestania, W.A., internal report, Aztec Mining Co Ltd, 12p (unpubl).

Mueller, A.G., 1988, Archaean gold-silver deposits with prominent calc-silicate alteration in the Southern Cross greenstone belt, Western Australia: Analogues of Phanerozoic skarn deposits. In Advances in understanding Precambrian gold deposits, Volume II. Edited by S.E. Ho and D.I. Groves. University of Western Australia, Nedlands, Geology Department and University Extension, Publication 12, p141-163.

Mueller, A.G., 1991, The Savage Lode magnesian skarn in the Marvel Loch gold-silver mine, Southern Cross greenstone belt, Western Australia. Part 1: Structural setting, petrography, and geochemistry. Canadian Journal of Earth Sciences, v. 28, p659-685.

Mueller, A.G. and Groves, D.I., 1991, The classification of Western Australian greenstone-hosted gold deposits according to wallrock-alteration mineral assemblages. Ore Geology Reviews, v. 6, p291-331.

Mueller, A.G., Groves, D.I. and Delor, C.P., 1991, The Savage Lode magnesian skarn in the Marvel Loch gold-silver mine, Southern Cross greenstone belt, Western Australia. Part 2: Pressure-temperature estimates and constraints on fluid sources. Canadian Journal of Earth Sciences, 28: p686-705.

Porter, D.J. and McKay, K.G., 1981, The nickel sulphide mineralization and metamorphic setting of the Forrestania area, Western Australia. Economic Geology, v. 76, p1524–1549.

Rutherford, R.A., 1991, Technical Report, Northern Estates EL 77/72 from 1.1.89 to 31.12.90, internal report No. 556, Aztec Mining Co Ltd (unpubl).

Turner, F.J., 1981, Metamorphic Petrology, Mineralogical and Field Aspects. McGraw Hill publ., 403pp.

APPENDIX I

EQUAL ANGLE, WULFF NET PROJECTIONS OF FABRICS
AND STRUCTURES MEASURED FROM ORIENTED CORE
(MD77, MD78, MD79, MD84, MD85A, MD88, MD88A)
AND PIT EXPOSURES IN THE BOUNTY MINE

Equal Angle

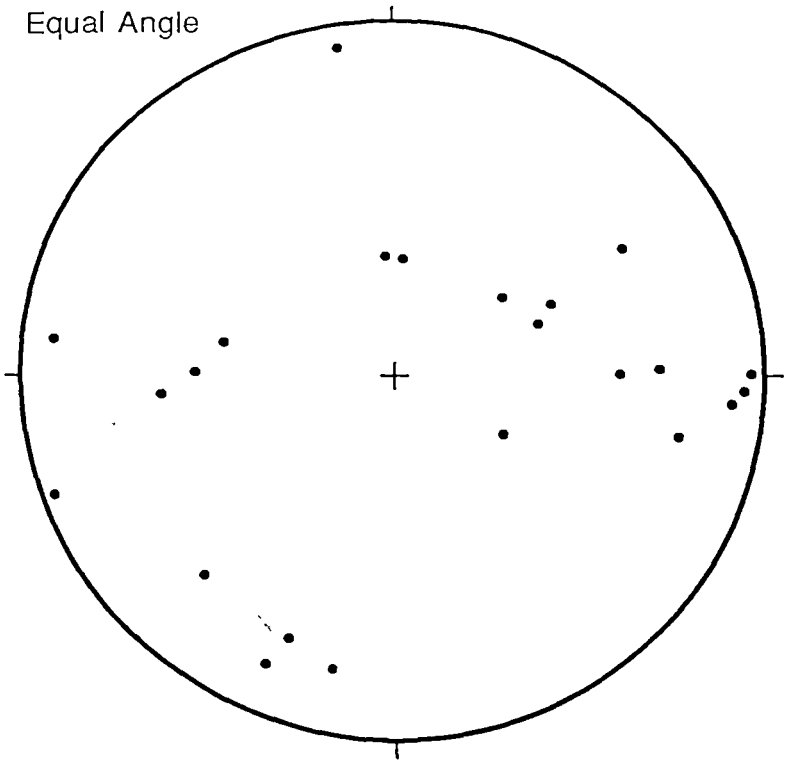

So N= 23

Equal Angle

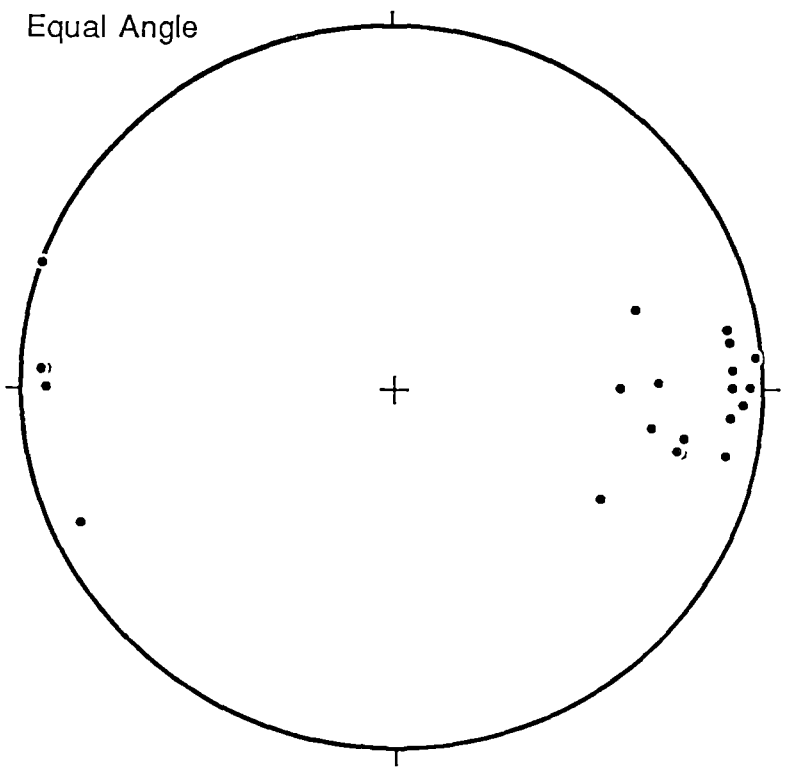

Mean vector 17° towards 94°

Sn N = 22

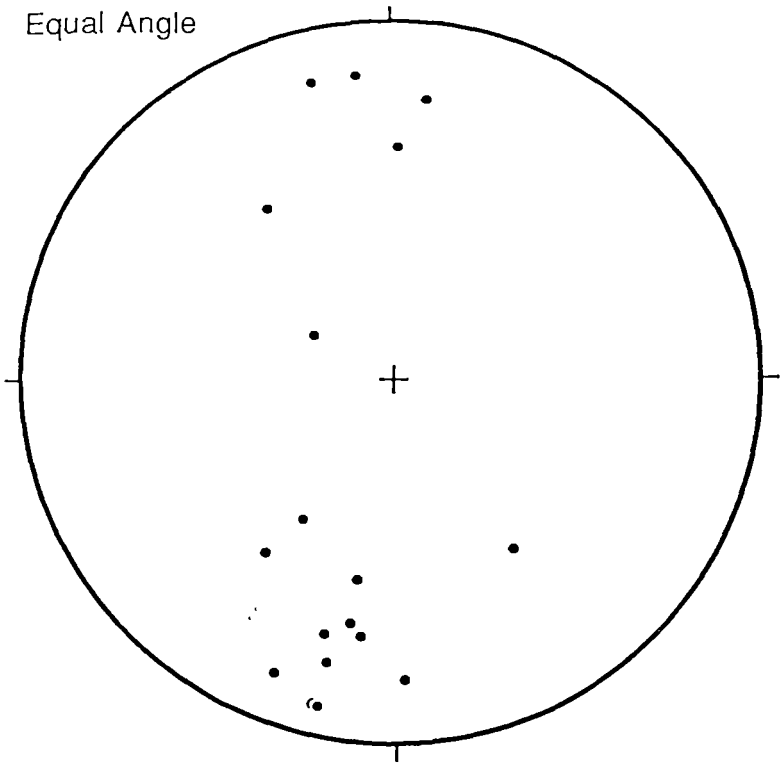

Fn axes with west-down normal profiles
N = 18

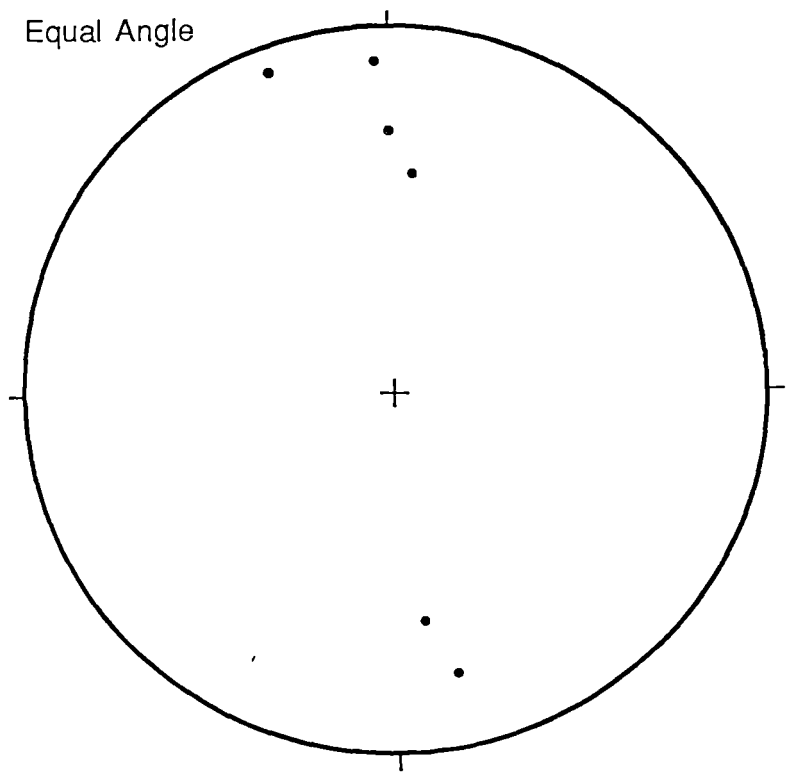

Fn axes with east-down normal profiles
N = 6

Equal Angle

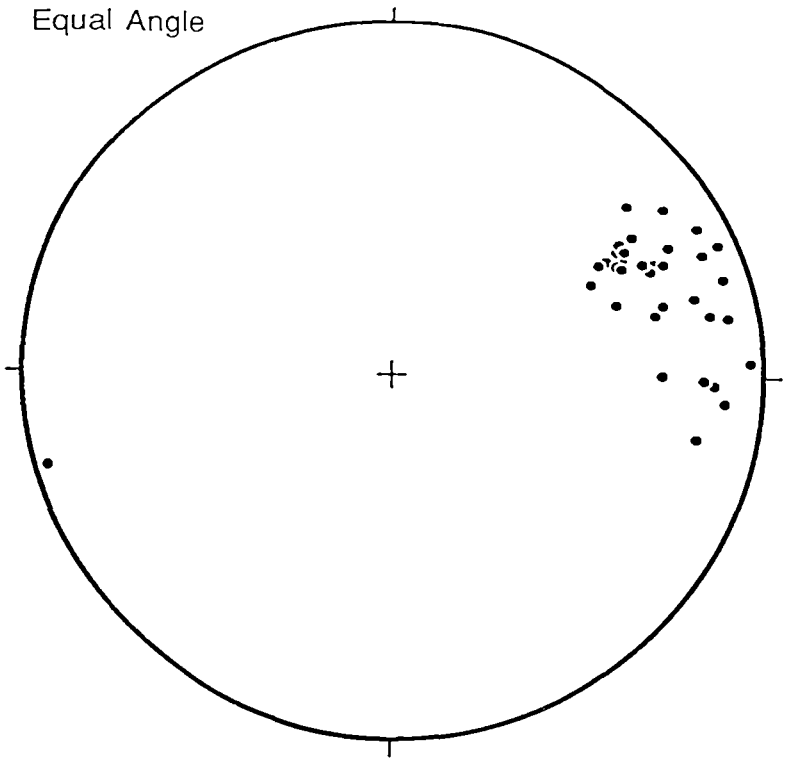

Mean vector 15° towards 70.6°

Sn + 1 N = 35

APPENDIX II

BOUNTY HORIZON CROSS SECTION 34920N SHOWING ITS STRUCTURAL ZONATION, GOLD GRADES AND PERCENTAGE PYRRHOTITE AND PYRITE

APPENDIX III

CONTOURED LONG SECTIONS OF THE SHEARED
HANGING WALL BOUNDARY OF THE BOUNTY HORIZON

PLAN No.	TITLE
8–1000–45	Form Diagram
8–1000–44	Changes in Strike
8–1000–42	Changes in Apparent Dip Angle
8–1000–43	Grade Contour Diagram